POSTER SESSION

1. Efficient generation of squeezed states of light based on modes with orbital angular momentum in a cavity configuration
2. Dynamics of the uncertainty value of quadratures for bosonic quantum states
3. Quantum state detection fidelity optimization for the ytterbium optical qubit
4. Using linear and nonlinear methods to reduce the error of quantum teleportation
5. Quantum memory based OAM single qudits multidimentional gates
6. Qudit-based quantum compiler
7. Photon pairs generation by frequency cascaded up-conversion of parametric down-conversion
8. Wigner function representation and efficient calculation method
9. Schrödinger cat states decoherence in a fiber quantum channel and their discrimination
10. Implementation of Optical Quantum Memory in a Tm:YAG Crystal Waveguide
11. Reconstructing linear-optical integrated circuits parameters through measurements of correlation functions of thermal fields
12. Implementation of revival of silenced echo memory protocol in $^{167}Er^{3+}$:Y_2SiO_5 crystal
13. Measurement of the normalized second-order correlation function for by photon fields by analog detectors
14. Atom chip for quantum sensing
15. Matrix permanents in statistical physics of many-body quantum systems
16. Countermeasure to laser damage attack (LDA) based on neutral-density filter
17. Nanoindentation-based approach to integration of quantum emitters in 2D materials with nanophotonic structures

Voronovo, Moscow, Russia November 9–12, 2021
4th International School on Quantum Technologies

Efficient generation of squeezed states of light based on modes with orbital angular momentum in a cavity configuration

E. N. Bashmakova*, **E.A. Vashukevich, T.Yu. Golubeva, Yu.M. Golubev**

St. Petersburg State University, St. Petersburg, Russia
*E-mail: bashmakova.elizaveta@mail.ru

Abstract

One of the essential practical challenges for quantum-optical and information applications is the efficient generation of squeezed states of light. In this work, we study the possibility of increasing the efficiency of the generation of states based on modes with orbital angular momentum in the parametric down conversion of light due to the optimal choice of the cavity configuration. Using the apparatus of the Heisenberg-Langevin equations for the eigenmodes of the system, we investigated the threshold values of the modes, obtained the optimal parameters of the cavity configuration for generating squeezed states, and estimated the highest degree of squeezing in the system.

Today, interest in squeezed states [1, 2] is associated with their relevance in quantum-optical and information applications, for example, in the construction of multipartite entangled (cluster) states for one way computations in continuous variables [3, 4]. One of the promising ways to obtain a set of squeezed multipartite states is to use the Laguerre-Gaussian modes with orbital angular momentum (OAM) [5, 6]. The main advantage of using the Laguerre-Gaussian modes is that the OAM projection can take any integer values, making it possible to work in a high-dimensional Hilbert space. For analyzing the quantum properties of the system, it is necessary to investigate the most interesting - the near-threshold region because it is in this region that the highest degree of squeezing can be observed.

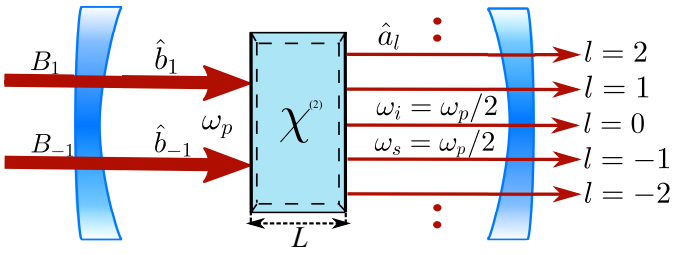

Figure 1: The schematic draw of the system under consideration: a crystal with a quadratic nonlinearity $\chi^{(2)}$, which ensures type-I phase synchronism, is placed in a cavity with spherical mirrors. The pump consists of two spatial Laguerre-Gaussian modes with OAM equal to +1 and -1. A multimode field is generated in the cavity with different values of the OAM but at the same frequency $\omega_p/2$.

This work considers a scheme for generating multipartite quantum states of light upon two-component pump of a parametric crystal in a cavity by two Laguerre-Gaussian beams with OAM equal to 1 and -1. The below-threshold operating mode of the optical parametric oscillator makes it possible to neglect the pump exhaustion in the theoretical description of parametric process. The efficiency of the generation of squeezed states and the correlation properties of the system are determined by the coupling parameters, which depend on the overlap of the transverse mode profiles. This dependence allows us to control the coupling parameters by changing the geometry of the fields by varying the cavity configuration. We aim to research the influence of the signal and pump modes waist widths ratio on generating quantum states of light with the highest degree of squeezing.

When identifying the eigenmodes of the system, the so-called supermodes [7], we demonstrate that different modes have different threshold values and have different degrees of squeezing. It can be shown that the first of the five distinguishable eigenmodes, in contrast to the others, remains in a vacuum state during the system's evolution. Moreover, the quadratures are equally squeezed or stretched in pairs (second and third, fourth and fifth).We want to determine the scheme's parameters that provide

the maximum degree of squeezing in the system. The most interesting case is when the generation's thresholds for two pairs of modes approach each other since it is in the near-threshold region that radiation's most pronounced quantum properties can be observed.

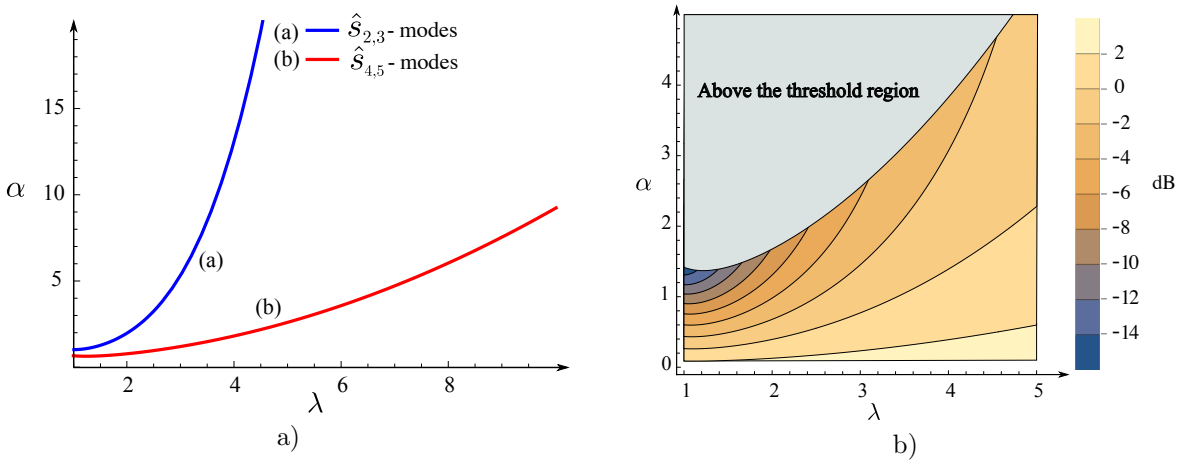

Figure 2: a) Dependence of the generation's threshold α on the ratio of the waist widths of the idler mode and the pump mode λ for different pairs of modes; b) the dependence of the spectrum power of quadratures' fluctuation when approaching the generation's threshold on the λ coefficient and the threshold parameter α.

We select the control parameter λ, which is determined by the ratio of the waist widths of the detected idler mode and the pump mode. The coefficient α characterizes the threshold parameters of supermodes. As it could be seen from Fig.2 a the behavior of the generation threshold depending on the geometric parameter λ. With a decrease in λ, the threshold values for different modes become closer. At the same time, with an increase in this ratio, the values of the threshold parameters increase, but at different rates. It is seen from Fig. 2 b the behavior of the minimum of spectrum power of the quadrature depending on the threshold value α and the geometric parameter λ. It is shown that the minimum values of spectral power of fluctuation are achieved in the limit of equality of the waist widths.

We demonstrate that the region of the most efficient generation of squeezed states is a configuration with the same values of the waist widths of the pump mode and the generated cavity modes. In this region, the thresholds for the generation of the same for all modes approach each other. The theoretically possible degree of squeezing in this region is -15.85 dB.

This work was supported by RFBR (grants 19-02-00204 and 19-32-90059).

References

[1] *U. L. Andersen, T. Gehring, C. Marquardt, G. Leuchs*, 30 years of squeezed light generation. Phys. Scripta. **91**, 053001 (2016).

[2] *S.L. Braunstein, P. van Loock*, Quantum information with continuous variables. Rev. Mod. Phys. **77**, 513 (2005).

[3] *R. Raussendorf, H.J. Briegel*, A one-way quantum computer. Phys. Rev. Lett. **86**, 5188 (2001).

[4] *H. Briegel, D. Browne, W. Dur, R. Raussendorf, M. Nest*, Measurement-based quantum computation. Nat.Phys. **5**, 19 (2009).

[5] *S.J. van Enk, G. Nienhuis*, Spin and orbital angular momentum of photons. EPL. **25**, 497 (1994).

[6] *G. Nienhuis, L. Allen*, Paraxial wave optics and harmonic oscillators. Phys. Rev. A. **48**, 656 (1993).

[7] *R. Medeiros de Araújo, J. Roslund, Y. Cai, G. Ferrini, C. Fabre, N. Treps*, Full characterization of a highly multimode entangled state embedded in an optical frequency comb using pulse shaping. Phys. Rev. A. **89**, 053828 (2014).

Voronovo, Moscow, Russia November 9–12, 2021
4th International School on Quantum Technologies

Dynamics of the uncertainty value of quadratures for bosonic quantum states

Svetlana Medvedeva[1*], Andrei Gaidash[1,2], George Miroshnichenko[3], Alexei Kiselev [2,4,5] , and Anton Kozubov[1,2]

[1] *Laboratory of Quantum Processes and Measurements, ITMO University, Saint Petersburg, Russia*
[2] *Department of Mathematical Methods for Quantum Technologies, Steklov Mathematical Institute of Russian Academy of Sciences, Moscow, Russia*
[3] *Faculty of Laser Photonics and Optoelectronics, ITMO University, Saint Petersburg, Russia*
[4] *Faculty of Photonics and Optoinformatics, ITMO University, Saint Petersburg, Russia*
[5] *5Faculty of Physics, St. Petersburg State University, St. Petersburg, Russia*
*E-mail: *ss_medvedeva@itmo.ru*

Abstract

We consider the time evolution of the mean values of the first and second moments of the quadrature operators for an arbitrary quantum state in a single mode transmitted through an optical fiber channel. Utilizing the density matrix formalism and the quantum optics theory we derive expressions for the dynamics of mentioned field observables for such prominent quantum states as squeezed vacuum state, squeezed coherent state and superposition of coherent states.

One of the main constraints on the technological utilization of the unique quantum features such as superposition or squeezing lies in decoherence: the detrimental influence of environment leads any quantum system to the loss of its beneficial quantum features [1]. A theory that may be employed to investigate the evolution of quantum systems considering decoherence is open quantum systems approach [2]. Within this theory different methods are being used, in our research we focus on solving a master equation for a density matrix of a quantum state.

Method

In order to give a description of a nonunitary dynamics of a bosonic quantum state study the Liouville master equation that is a special case of the Gorini–Kossakowski–Sudarshan–Lindblad (GKSL) master equation equation [3]. The explicit solution to this equation may be found, for example, with the use of SU(1,1) algebra formalism [4], Jordan mapping [5]. In this investigation we act by an operator of interest ($\hat{A}$, for example) on the master equation, apply the trace operation, like in Equation (1), and then solve the resulting equation to obtain the time-dependence of a mean value of an operator [6, 7].

$$\mathrm{Tr}\left\{\frac{\partial}{\partial t}\hat{A}\hat{\rho}\left(t\right)\right\} = -i\,\mathrm{Tr}\left\{\hat{A}\left[\hat{H},\hat{\rho}\left(t\right)\right]\right\} + \mathrm{Tr}\left\{\hat{A}\hat{\Gamma}\hat{\rho}\left(t\right)\right\} \rightarrow \left\langle\hat{A}\left(t\right)\right\rangle. \tag{1}$$

Results

Utilizing the method presented above We obtain the expressions of time evolution for the first and second moments of the quadrature operators [8] for an arbitrary bosonic quantum state in a single mode transmitted through an optical fiber channel. Moreover, we derive an expression of the dynamics of the uncertainty value of the quadrature operators for an arbitrary bosonic quantum state. We perform a numerical simulation of the obtained time evolution for squeezed vacuum state, squeezed coherent state and superposition of coherent states, see Fig. 1.Fig. 2, investigating the dependence of the dynamics on the squeezing parameter and other characteristics of quantum states.

This work was supported by the Ministry of Science and Education of the Russian Federation (Passport #2019-0903).

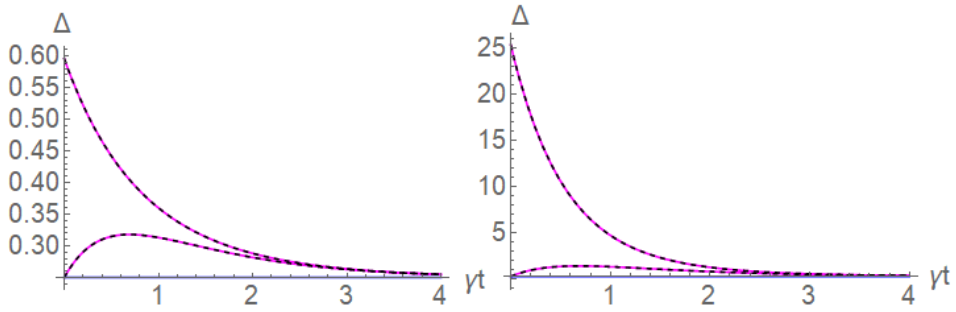

Figure 1: The envelope function of the dynamics of the uncertainty value Δ for a squeezed vacuum state (purple) and squeezed coherent state (black) for different values of squeezing parameter.

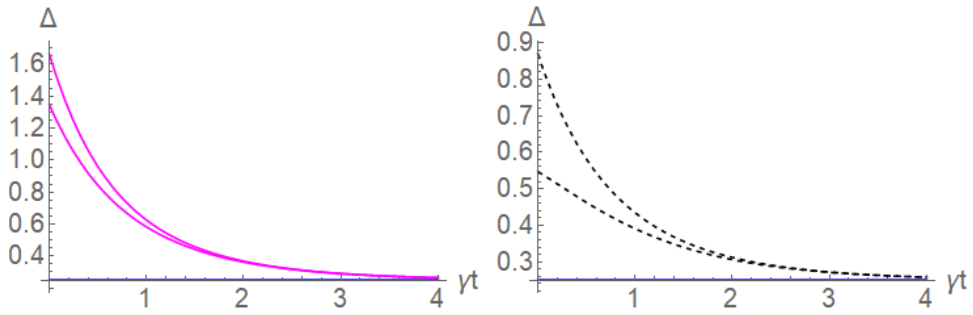

Figure 2: The envelope functions of the dynamics of the uncertainty value Δ for a superposition of coherent states with different values of phase difference.

References

[1] *H.-P. Breuer, F. Petruccione*, The theory of open quantum systems. Oxford University Press on Demand. (2002).

[2] *E. Joos,H. D. Zeh, C. Kiefer, D. J. Giulini, J. Kupsch, I. O. Stamatescu* , Decoherence and the appearance of a classical world in quantum theory. Springer Science & Business Media. (2013).

[3] *H. Carmichael*, An open systems approach to quantum optics: lectures presented at the Université Libre de Bruxelles, October 28 to November 4, 1991. Springer Science & Business Media. **18**, (2009).

[4] *A.A. Gaidash, A.Kozubov. Kozubov, G.P. Miroshnichenko*, Dissipative dynamics of quantum states in the fiber channel. Physical Review A **102**, 2, 023711 (2020).

[5] *A.A. Gaidash, A.V. Kozubov, G.P. Miroshnichenko, A.D. Kiselev*, Quantum dynamics of mixed polarization states: effects of environment-mediated intermode couplings. Optical Society of America **38**, 9, 2603-2611 (2021).

[6] *A.A. Gaidash, A.V. Kozubov, S.S. Medvedeva, G.P. Miroshnichenko*, The Influence of Signal Polarization on Quantum Bit Error Rate for Subcarrier Wave Quantum Key Distribution Protocol. Multidisciplinary Digital Publishing Institute **22**, 12, 1393 (2020).

[7] *S.S. Medvedeva, A.A. Gaidash, A.V. Kozubov, G.P. Miroshnichenko*, Dynamics of field observables in quantum channels. IOP Publishing **1984**, 1, 012007 (2021).

[8] *M. O. Scully, M. S. Zubairy*, Quantum optics. American Association of Physics Teachers. (1999).

Voronovo, Moscow, Russia November 9–12, 2021
4th International School on Quantum Technologies

Quantum state detection fidelity optimization for the ytterbium optical qubit

Nikita Semenin[1,2*], **Alexander Borisenko**[1,2],
Ilya Zalivako[1], **Ilya Semerikov**[1],
Ksenia Khabarova[1,2,3], **Nikolay Kolachevsky**[1,3]

[1] *Lebedev Physical Institute of the RAS, Moscow, Russia*
[2] *Moscow Institute of Physics and Technology, Dolgoprudny, Russia*
[3] *Russian Quantum Center, Skolkovo, Russia*
*E-mail: semeninnv@gmail.com

Abstract

A theoretical model of the state detection process for the optical qubit in the $^{171}Yb^{+}$ ion, based on a laser cooling system, was developed. Analytical expressions for the state detection fidelities considering dark photon counts are derived. A numerical optimization of the experimental parameters was carried out. An upper fidelity limit of 99.4% was found and attributed to the transient process at the start of the measurement procedure. The characteristic values of the detection parameters are given, which ensure sufficient proximity to the optimal fidelity value.

Ultracold trapped ions remain one of the most rapid-growing and promising platforms for quantum computation. Their strong Coulomb interaction, combined with the ability to precisely manipulate them using laser radiation, offer relatively fast and highly efficient implementations of elementary quantum procedures, such as entanglement, quantum state preparation and detection. One of these procedures, namely state detection, is considered in more detail in the presentation with respect to the optical qubit in the $^{171}Yb^{+}$ ion.

The laser system that is used for Doppler cooling of the ion can also be utilized for quantum state detection in an ion optical qubit due to its state-dependent fluorescence (fig. 1). In the presentation we use the rate-equation approach to develop a theoretical model of the detection process in this system. This model can then be used to derive the photon statistics [1], as well as the expressions for the state detection fidelities (for both qubit states) as a function of atomic and experimental parameters, such as detection time, laser intensities, photon collection efficiency, dark count rate and discriminator threshold [2]. These parameters have then been numerically optimized so as to achieve the maximal fidelity value. It turns out that for each dark count rate and photon collection efficiency there are unique values for the detection time and the discriminator threshold.

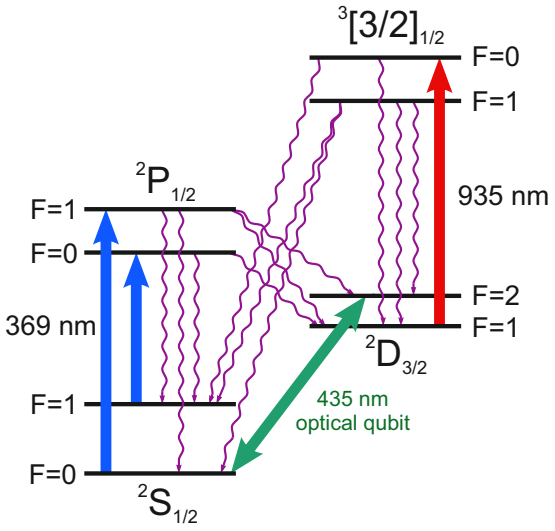

Figure 1: $^{171}Yb^{+}$ optical qubit state detection scheme. Wavy arrows represent allowed decay transitions.

For the detection scheme considered here, the optimal fidelity approaches a limit of 99.4% as the photon collection efficiency increases (fig. 2). This limit is independent of the experimental parameters and exists because of the transition process that takes place at the beginning of detection, which partially pumps the ion from one qubit state to another with the probability of 0.6%, correspondingly lowering the fidelity by that much.

The characteristic values of the photon collection efficiency, at which the fidelity is sufficiently close to the limit, does depend on experimental parameters, especially on the dark count rate, such that more efficient photon collection is required for higher dark count rates. However, for reasonable dark count levels the sufficient collection efficiency does not exceed 1 percent, which is easily achievable with modern optics.

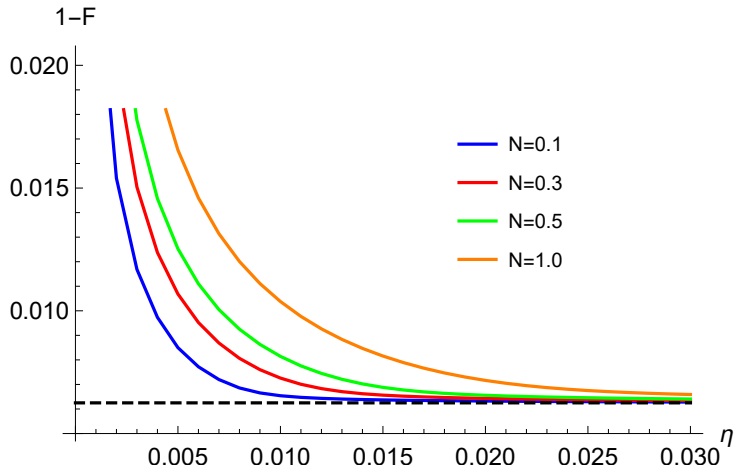

Figure 2: Optimal infidelities as a function of the photon collection efficiency. The noise parameter N is proportional to the dark photon count rate. The dashed line indicates the 0.6% limit.

Acknowledgements

This work was supported by the Russian Science Foundation (grant №19-12-00274) and the Russian Foundation for Basic Research (grant №20-32-90020).

References

[1] *M. Acton, K.A. Brickman, P.C. Haljan, P.J. Lee, L. Deslauriers and C. Monroe*, Near-perfect simultaneous measurement of a qubit register. Quantum Information & Computation **6**, 465 (2006).

[2] *N.V. Semenin, A.S. Borisenko, I.V. Zalivako, I.A. Semerikov, K.Y. Khabarova and N.N. Kolachevsky*, Quantum state detection fidelity optimization for the $^{171}Yb^{+}$ optical qubit. JETP Letters **114**, 557 (2021).

Voronovo, Moscow, Russia November 9–12, 2021
4th International School on Quantum Technologies

Using linear and nonlinear methods to reduce the error of quantum teleportation

E. R. Zinatullin*, **S. B. Korolev**, **T. Yu. Golubeva**

St. Petersburg State University, St. Petersburg, Russia
*E-mail: e.r.zinatullin@mail.ru

Abstract

We have investigated linear and nonlinear methods for reducing the error of quantum teleportation. We have shown that the CZ operation leads to the lower error of teleportation. This error can be further reduced by choosing appropriate weight coefficients for the CZ transforms. We propose a modified quantum teleportation scheme to increase the teleportation accuracy by applying a cubic phase gate to the displaced squeezed state. We show that it allows achieving less error than the original scheme with sufficient displacement of the resource squeezed state.

Quantum teleportation is one of the basic protocols of quantum information processing [1, 2]. It is this protocol that underlies one of the promising models of universal quantum computation – the one-way quantum computation model [3, 4]. In our work, we discuss the continuous-variable quantum teleportation protocol. Unlike discrete quantum systems, the use of continuous-variable ones allows one to build deterministic schemes. However, working with continuous-variable quantum systems also has a significant drawback: the presence of unavoidable errors associated with the finite squeezing degree of states, which are used as a resource for teleportation. Continuous-variable one-way quantum computation has inherited this disadvantage. The squeezing, which is experimentally achievable at the moment, turns out to be insufficient for performing fault-tolerant universal one-way quantum computations: the maximum experimentally achievable squeezing degree is -15 dB [5], whereas for such computations (without using surface codes and a postselection procedure) the squeezing of -20.5 dB [6] is required. In this regard, the reduction of unavoidable errors for continuous-variable quantum computation remains an important theoretical problem.

We have compared two entangling transformations: CZ gate and mixing signals on the beam splitter [7]. We tested the quality of these transformations in terms of adding an error under the teleportation protocol. We have shown that employing the CZ gate brings in lower noise, thus providing a higher quality of protocol performance. By replacing the beam splitters with CZ transforms, we were able to reduce the error in one of the quadratures by using the weight coefficients of the CZ transformations [8]. This conclusion is valid not only for an idealized CZ scheme but also for a real one, for example, for an optical CZ gate [9] in some range of reflection coefficient values (Fig. 1). Thus, it is possible to increase the fidelity of teleportation while remaining within the framework of Gaussian deterministic operations.

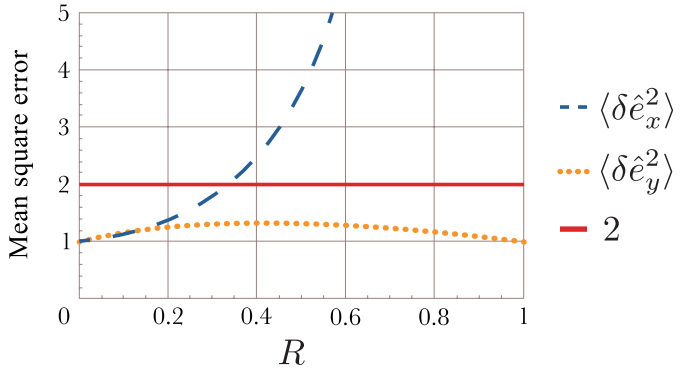

Figure 1: Mean-square errors of the quadratures of teleported signal, depending on the reflection coefficient of the beam splitters used in the optical CZ gates. The solid red line indicates the noise level of teleportation in the original scheme with the beam splitters.

Another way to improve the accuracy of teleportation is to use non-Gaussian states as the main resource. As such a resource, you can use the states obtained using the procedure of conditional subtraction or addition of photons applied to the Gaussian entangled state [10]. However, this procedure is probabilistic, which means that a teleportation protocol using such non-Gaussian states will no longer be deterministic.

In this regard, we modified the CZ transform teleportation scheme proposed earlier using a cubic phase gate [11] to reduce the error in both quadratures (see Fig. 2). We have shown that it is possible to reduce the teleportation error in one of the quadratures using a cubic phase gate [12]. We have demonstrated this by analyzing our scheme in terms of adding a teleportation error in the Heisenberg picture. In addition, we have described the scheme in the Schrödinger picture and have demonstrated that, to fulfill the approximations made by us, it is necessary to perform relatively small displacements of the squeezed state before applying the cubic phase transformation. These displacements can be implemented in practice.

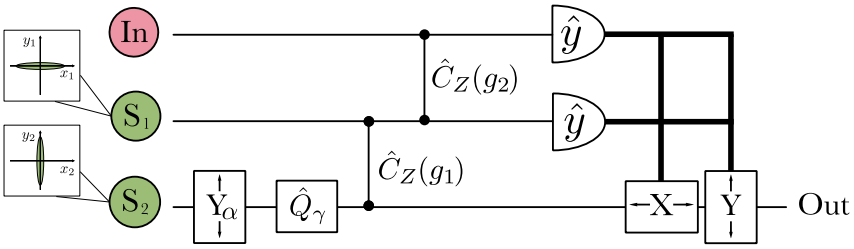

Figure 2: Teleportation scheme using a cubic phase gate. In the diagram, In is the input (teleported) state; S_1 and S_2 are oscillators squeezed in orthogonal quadratures; Y_α denotes the displacement of the y quadrature by a fixed value α; $\hat{Q}_\gamma$ is a cubic phase gate with a conversion coefficient γ; $\hat{C}_Z(g_i)$ is CZ transformations with weight coefficients g_i; $\hat{y}$'s are homodyne detectors measuring the y quadrature of the field in the channel; and X and Y denote devices that displace the corresponding quadratures of the fields in the channel, depending on the detection results.

This work was financially supported by the Russian Foundation for Basic Research (Grant No. 19-02-00204a) and Theoretical Physics and Mathematics Advancement Foundation "BASIS" (Grant No. 21-1-4-39-1).

References

[1] *S. L. Braunstein and H. J. Kimble*, Phys. Rev. Lett. **80**, 869 (1998).

[2] *A. Furusawa, J. L. Sørensen, S. L. Braunstein, C. A. Fuchs, H. J. Kimble, and E. S. Polzik*, Science **282**, 706 (1998).

[3] *N. C. Menicucci, P. van Loock, M. Gu, C. Weedbrook, T. C. Ralph, and M. A. Nielsen*, Phys. Rev. Lett. **97**, 110501 (2006).

[4] *R. Raussendorf and H. J. Briegel*, Phys. Rev. Lett. **86**, 5188 (2001).

[5] *H. Vahlbruch, M. Mehmet, K. Danzmann, and R. Schnabel*, Phys. Rev. Lett. **117**, 110801 (2016).

[6] *N. C. Menicucci*, Phys. Rev. Lett. **112**, 120504 (2014).

[7] *E. R. Zinatullin, S. B. Korolev, and T. Yu. Golubeva*, Phys. Rev. A **103**, 062407 (2021).

[8] *M. V. Larsen, J. S. Neergaard-Nielsen, and U. L. Andersen*, Phys. Rev. A **102**, 042608 (2020).

[9] *J.-i. Yoshikawa, Y. Miwa, A. Huck, U. L. Andersen, P. van Loock, and A. Furusawa*, Phys. Rev. Lett. **101**, 250501 (2008).

[10] *T. Opatrný, G. Kurizki, and D.-G. Welsch*, Phys. Rev. A **61**, 032302 (2000).

[11] *D. Gottesman, A. Kitaev, and J. Preskill*, Phys. Rev. A **64**, 012310 (2001).

[12] *E. R. Zinatullin, S. B. Korolev, and T. Yu. Golubeva*, Phys. Rev. A **104**, 032420 (2021).

Voronovo, Moscow, Russia November 9–12, 2021
4th International School on Quantum Technologies

Quantum memory based OAM single qudits multidimentional gates

Baeva A.V.*, **Vashukevich E.A., Golubeva T.Yu., Golubev Yu.M.**

St Petersburg State University, 7/9 Universitetskaya nab., 199034, St. Petersburg, 199034 Russia
*E-mail: alexandrabaeva@mail.ru

Abstract

We propose a method for implementing multidimensional quantum gates for OAM single qudits based on the transformation of light modes with OAM in the Raman quantum memory scheme. We describe a way of encoding the logical qudits which ensures cyclically closed transformations. The characteristics of the quantum gate $\hat{X}_d$ such as fidelity and success probability for qudits of different dimensions are numerically calculated. We show the estimation of the transformation effectiveness, taking the information capacity of the channel into account.

In recent years, the interest in using multilevel quantum systems (qudits) for quantum computing and quantum communication is significantly increased. The qudits, as multilevel quantum systems of dimension $d \geq 3$, have several considerable advantages compared to the qubit system with $d = 2$. For example, in work [1], it was shown that one qudit with eight levels could replace a system of three qubits. Moreover, in qudit-based quantum cryptography protocols [2] the security of the protocol increases with the dimension of the system.

Many variants of physical systems have been proposed for qudit encoding, such as time-bin [3], multiphoton polarization states [4], the orbital angular momentum of light (OAM) [5]. The latter being of particular interest because of several reasons. Firstly, the Laguerre-Gaussian modes with OAM are well localized and stable to effects of external distortion. Secondly, the OAM can take any integer values, allowing us to work in a high-dimensional Hilbert space [6]. As for today, some attempts to construct quantum logic gates for OAM qudits were made. In the work [7], authors demonstrate the experimental realization of gates $\hat{X}_d$ in the case of qudits of dimension $d = 4$ and achieve the high values of the gate's efficiency ≈ 0.9. However, the problem of constructing single qudit gates that transform a quantum state of light with an OAM of arbitrary dimension in a controlled manner with high fidelity and efficiency is still open. In this work, we propose an alternative mechanism for constructing $\hat{X}_d$ gates, assuming that $\hat{Z}_d$ gates can be relatively easily obtained using the Dove prism [8].

In the work [9], the transformation of the OAM of light in the scheme of Raman quantum memory on cold atoms was proposed. We obtained the specific values of the system's parameters such that the modes of the quantum field with different OAM interact with the atomic ensemble independently of each other. In this case, the interaction efficiency is determined by the overlap integral of the transverse profiles of Laguerre-Gaussian modes and, therefore, can be controlled by varying the spatial profile of the driving field at the writing and read-out stages. The possibility of such control allows us to achieve sufficiently high efficiency values (≈ 0.9).

Using transformation, described above, we construct quantum single-qudit gates $\hat{X}_d^m$, where m are integer powers of the operator $\hat{X}_d$, for OAM of qudits of different dimensions [10]. The main goal was in constructing the transformation with several essential properties: high probability, high fidelity and coherence. It means that the quantum gate should act on the qudit state, consistently transforming each term of the superposition. The calculation of the success probability of the gates $\hat{X}_3^m$ for the special case of the qudit dimension $d = 3$ showed that the probability of the conversion with adding an OAM quanta increases with the value of l. At the same time, in the case of subtracted OAM quanta ($m = -1, -2$), a higher probability can be achieved in the region of small values of l (see Fig. 1), which seems to be an important advantage since small OAM values could be more easily experimentally achieved than large ones. It should be noted that all these transformations with an exceptionally high level of fidelity (with infidelity value about 10^{-5}). Remarkably, a specific value of the control parameter z_s/z_R (the normalized relative shift of the beam waists of the driving and quantum fields), which provides high probabilities over a wide range of l values, could be calculated for each transformation.

We have also estimated the optimal dimension of the qudit for performing the calculations with the proposed gate. A comparison of the characteristics of the gates $\hat{X}_d^{-1}$ and $\hat{X}_d^{-2}$ for different dimensions

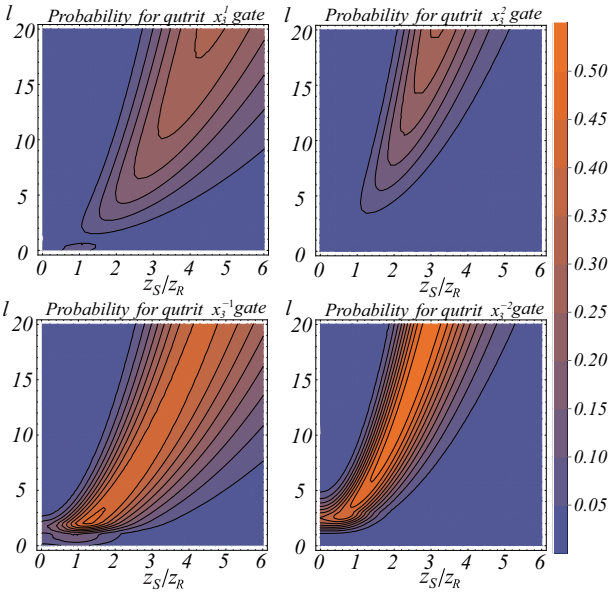

Figure 1: The probabilities of success of the qutrite gates $\hat{X}_3$, $\hat{X}_3^2$ (top), $\hat{X}_3^{-1}$, $\hat{X}_3^{-2}$ (bottom) depending on the values l and the parameter z_s/z_R (the normalized relative shift of the beam waist of the driving and quantum fields) that controls the geometry of the modes.

showed that in our scheme, the preferable qudit's dimensions is $d = 3$ and $d = 4$, since for these values the gain in the channel's information capacity, increasing with the qubit dimension, balance the decreasing with dimension success probability.

The reported study was supported by RFBR (Grants No. 19-32-90059, 19-02-00204) and Theoretical Physics and Mathematics Advancement Foundation "BASIS" (Grant 20-1-5-120-1).

References

[1] *E.O. Kiktenko, A.K. Fedorov, O.V. Man'ko and V.I. Man'ko*, Multilevel superconducting circuits as two-qubit systems: Operations, state preparation, and entropic inequalities. Phys. Rev. A **91**, 042312 (2015).

[2] *L. Sheridan and V. Scarani*, Security proof for quantum key distribution using qudit systems. Phys. Rev. A **82**, 030301 (2010).

[3] *H. Bechmann-Pasquinucci and W. Tittel*, Quantum cryptography using larger alphabets. Phys. Rev. A **61**, 062308 (2000).

[4] *Y.I. Bogdanov, M.V. Chekhova, S.P. Kulik, G.A. Maslennikov, A.A. Zhukov, C.H. Oh and M.K. Tey* , Qutrit state engineering with biphotons. Phys. Rev. Lett. **93**, 230503 (2004).

[5] *N. Bent, H. Qassim, A.A. Tahir, D. Sych, G. Leuchs, L.L. Sánchez-Soto, E. Karimi and R.W. Boyd*, Experimental realization of quantum tomography of photonic qudits via symmetric informationally complete positive operator-valued measures. Phys. Rev. X **5**, 041006 (2015).

[6] *L. Allen, M.W. Beijersbergen, R.J.C. Spreeuw and J.P. Woerdman*, Orbital angular momentum of light and the transformation of Laguerre-Gaussian laser modes. Phys. Rev. A, **45**, 8185 (1992).

[7] *A. Babazadeh, M. Erhard, F. Wang, M. Malik, R. Nouroozi, M. Krenn and A. Zeilinger*, High-dimensional single-photon quantum gates: concepts and experiments. Phys.Rev. Lett. **119**, 180510 (2017).

[8] *Y. Zhang, F.S. Roux, T. Konrad, M. Agnew, J. Leach, and A. Forbes*, Engineering two-photon high-dimensional states through quantum interference. Science advances, **2**, e1501165 (2016).

[9] *E.A. Vashukevich, T.Y. Golubeva, and Y.M. Golubev* Conversion and storage of modes with orbital angular momentum in a quantum memory scheme. Physical Review A, **101**, 033830. (2020).

[10] *E.A. Vashukevich, T.Y. Golubeva, and Y.M. Golubev* High-fidelity quantum gates for OAM qudits on quantum memory. arXiv preprint arXiv:2105.12178 (2021).

Voronovo, Moscow, Russia November 9–12, 2021
4th International School on Quantum Technologies

Qudit-based quantum compiler

A.S. Nikolaeva[1,2*], **E.O. Kiktenko**[1,2,3], **A.K. Fedorov**[1,2]

[1] *Russian Quantum Center, Skolkovo, Moscow 143025, Russia*
[2] *Moscow Institute of Physics and Technology, Dolgoprudny, Moscow Region 141700, Russia*
[3] *Steklov Mathematical Institute of Russian Academy of Sciences, Moscow 119991, Russia*
*E-mail: anastasiya.nikolayeva@phystech.edu

Abstract

We develop a qudit-based quantum compiler that employs two ways to work with qudits and allows us to implement quantum circuits on d-level quantum systems. It calculates the resources required to realize an input circuit and recommends the optimal technique for utilizing qudits' space. The proposed compiler is compatible with trapped-ion platform.

One of the major challenges in the development of quantum computers is the maintenance of quantum systems' coherent properties when they are scaled. Usually, the primary source of decoherence is the imperfection of two-qubit gates, which are based on organizing an accurate controlled interaction between physical objects. One of the ways for minimizing a required number of interactions for realizing quantum algorithms is utilizing the additional degrees of freedom of employed quantum information carriers that is going from qubits to qudits (d-dimensional quantum systems with $d \geq 3$).

In our work we develop a quantum compiler for qudit-based quantum processor that combines two approaches for working with qudits (see Fig. 1). The first approach is to use extra levels of qudits for substituting ancillary qubits. This approach is especially useful for decomposing multi-qubit gates (e.g. Toffoli and generalized Toffoli gates) into two-particle interactions [1, 2]. The second approach is to consider qudit's space as a space of multiple qubits [3]. This allows increasing an effective number of qubits for realization of quantum algorithms.

Given a 'high-level' input qubit circuit, consisting of some standard qubit gates, and information about available qudit-based hardware processor, the developed compiler outputs optimized qudit circuit, consisting of single-qudit and two-qudit gates, which is equivalent to the input one. Our compiler is compatible with trapped-ion quantum computing platform, having possibility to realize Mølmer–Sørensen gates within all-to-all topology of connections, and qudits of dimension $d = 3$. To realize the optimal qudit-based circuit realization, the compiler examines all possible mappings between qubits of the input circuits and qudits of the processor, and finds out the decomposition of the input circuit with the highest possible fidelity, given fidelities of single-qudit and two-qudit operations.

The developed qudit-based quantum compiler allows one to estimate the required resources to perform quantum algorithms and to identify the most preferred way to use the resource of qudits' higher levels. We test our qudit-based compiler with realistic parameters of trapped-ion-based quantum processor on four common quantum algorithms: Grover's search algorithm, Deutsch–Jozsa algorithm, Bernstein–Vazirani algorithm, and SWAP test. The results show that the greatest increase in fidelity, compared to straightforward realization with qubits, is observed in algorithms containing multi-qubit generalized gates, such as generalized Toffoli gate.

The research is supported by the grant UMNIK (Agreement 103GUCEC8-D3/56361 form 21.12.2019; development of the emulator of qudit-based quantum processors), and Leading Research Center on Quantum Computing (Agreement No. 014/20; compilation and optimization methods).

References

[1] *B.P. Lanyon, M. Barbieri, M.P. Almeida, T. Jennewein, T.C. Ralph, K.J. Resch, G.J. Pryde, J.L. O'Brien, A. Gilchrist, and A.G. White*, Nat. Phys. **5**, 134 (2009).

[2] *E. O. Kiktenko, A.S. Nikolaeva, P. Xu, G.V. Shlyapnikov, and A.K. Fedorov*, Physical Review A **101**, 022304 (2020).

[3] *E.O. Kiktenko, A.K. Fedorov, A.A. Strakhov, and V.I. Man'ko*, Phys. Lett. A **379**, 1409 (2015).

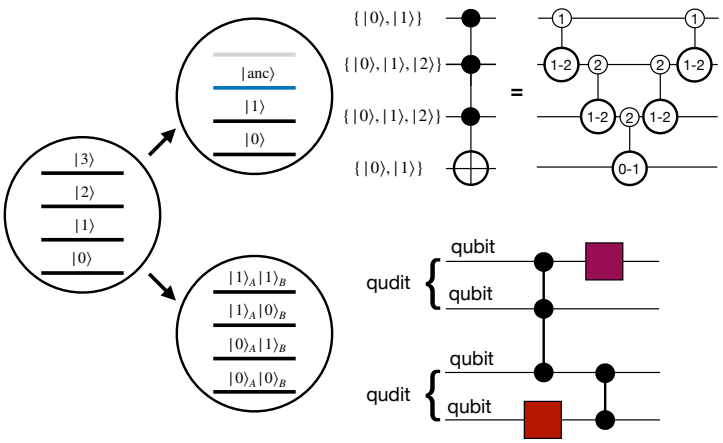

Figure 1: Two approaches to use qudits for quantum computing: (i) higher levels in qudits can be used as ancillary states for gate decompositions (the upper part of the picture), and (ii) the qudit's space can be considered as the space of several logical qubits for increasing effective number of qubits (the lower part on the picture).

Voronovo, Moscow, Russia November 9–12, 2021
4th International School on Quantum Technologies

Photon pairs generation by frequency cascaded up-conversion of parametric down-conversion

Andrei Rasputnyi[1*], **Denis Kopylov**[1]

[1] *Department of Physics, M.V. Lomonosov Moscow State University, Moscow, Russia*
*E-mail: andrey@shg.ru

Abstract

The generation of photon pairs by cascaded frequency up-conversion (CUpC) of spontaneous parametric down-conversion (SPDC) is theoretically studied. The output wave function of light is obtained using Wei-Norman technique with explicit accounting of wave-vector mismatches of SPDC and CUpC. The fulfilment of cascaded phase-matching conditions leads to the efficient and noiseless up-conversion of signal or idler photon and result in generation of IR-UV photon pairs using pump in visible spectral range in the single nonlinear crystal.

Second-order nonlinear processes are of great interest in quantum optics as they provide flexible experimental methods for non-classical fields generation and control [1]. The most acknowledged source of non-classical light is spontaneous parametric down-conversion (SPDC) which results in the decay of pump (p_1) photon in signal (s) and idler (i) photons with lower frequency [2]. In the case of weak pump, we obtain biphoton radiation which possesses quantum correlations that find large range of applications in quantum computation, metrology and imaging. The efficiency of SPDC crucially depends on wave-vector mismatch $\widetilde{\Delta} = k_{p_1} - k_s - k_i$, where k_{p_1}, k_s, k_i are wave-vectors of pump, signal and idler photons, respectively. The most efficient SPDC is observed when $\widetilde{\Delta} = 0$. Besides, signal and idler modes can be involved in additional nonlinear processes, such as cascaded up-conversion (CUpC) which occurs simultaneously with SPDC in the same nonlinear crystal [3]. This process results in creation of up-converted signal (us) and up-converted idler (ui) photons in the presence of additional pump (p_2) wave. CUpC of signal and idler photons are determined also by additional wave-vector mismatches $\Delta_s = k_{us} - k_s - k_{p_2}$, $\Delta_i = k_{ui} - k_i - k_{p_2}$. As a result using pump in visible range enables to up-convert signal (or idler) photon from infrared (IR) to ultraviolet (UV) spectral range. Thus we have to consider the spatial dynamics of four coupled modes (s, i, us, ui) in the nonlinear crystal to determine light properties of the output of the crystal. In [4] the new regime of coupled generation is found which leads to full up-conversion of signal or idler photons when cascaded phase-matching condition $\widetilde{\Delta} = \Delta_s \neq 0$ (or $\widetilde{\Delta} = \Delta_i \neq 0$) is satisfied.

In this work, we theoretically investigate the generation of photon pairs under the fulfilment of cascaded phase-matching condition. We implement Wei-Norman technique [5] using analytical solution of Heisenberg equation of annihilation operators that is found in form of Bogoluibov transformation [4] in order to calculate the output state of light in Schrodinger representation. In this way, we get exact expressions for probability amplitudes of photon pairs. The output state of light is described in four-mode Fock state basis

$$|\Psi\rangle = F_{\text{vac}}|\text{vac}\rangle + F_{s,i}|1_s, 1_i, 0_{us}, 0_{ui}\rangle + F_{us,i}|0_s, 1_i, 1_{us}, 0_{ui}\rangle + F_{s,ui}|1_s, 0_i, 0_{us}, 1_{ui}\rangle, \quad (1)$$

where F_{vac}, $F_{s,i}$, $F_{us,i}$, $F_{s,ui}$ are the probability amplitudes for vacuum state $|\text{vac}\rangle$ and for the photon pairs $|1_s, 1_i, 0_{us}, 0_{ui}\rangle$, $|0_s, 1_i, 1_{us}, 0_{ui}\rangle$, $|1_s, 0_i, 0_{us}, 1_{ui}\rangle$, respectively. We have omitted the rest of possible states as theirs probability amplitudes are much smaller than $F_{s,i}$, $F_{us,i}$, $F_{s,ui}$.

In Fig.1(a,b) the dependence of probabilities $|F_{s,i}|^2$, $|F_{us,i}|^2$ on wave-vector mismatches of SPDC $\widetilde{\Delta}$ and CUpC of signal photon Δ_s are shown. We can suppress probability $|F_{s,ui}|^2$ when $\Delta_i \gg \Delta_s$. The most efficient generation of SPDC pairs $|1_s, 1_i, 0_{us}, 0_{ui}\rangle$ is obtained, when phase-matching condition $\widetilde{\Delta} = 0$ is satisfied. As for the generation of photon pairs $|0_s, 1_i, 1_{us}, 0_{ui}\rangle$, there are two options: $\widetilde{\Delta} = 0$ and $\widetilde{\Delta} = \Delta_s$. In the first case, we obtain non-zero probability of SPDC photon pairs and pairs $|0_s, 1_i, 1_{us}, 0_{ui}\rangle$ which results in coincidence rate between signal-idler ($s-i$) and up-converted signal-idler ($us-i$) modes. Another option is to exploit cascaded phase-matching $\widetilde{\Delta} = \Delta_s$ when photon pairs $|0_s, 1_i, 1_{us}, 0_{ui}\rangle$ are

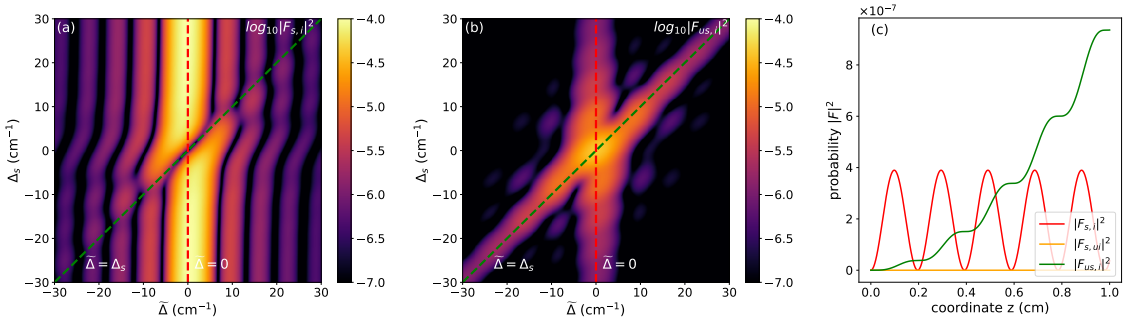

Figure 1: (a), (b)– probabilities $|F_{s,i}|^2$, $|F_{us,i}|^2$ of photon pairs generation, respectively (length of crystal $L = 1$ cm). (c)– dependence of probabilities $F_{s,i}$, $F_{us,i}$ on the length of crystal with the fulfillment of cascaded phase-matching condition $\widetilde{\Delta} = \Delta_s = 31$ cm^{-1}. For all plots wave-vector mismatch of CUpC of idler photon is $\Delta_i = 236$ cm^{-1}, parametric gain $\Gamma = 0.01$.

efficiently generated while the probability $|F_{s,i}|^2$ oscillates with detuning of wave-vector mismatch $\widetilde{\Delta}$. Then we obtain only IR-UV photon pairs $|0_s, 1_i, 1_{us}, 0_{ui}\rangle$ in the minima of $|F_{s,i}|^2$:

$$|\Psi\rangle = F_{\text{vac}}|\text{vac}\rangle + F_{us,i}|0_s, 1_i, 1_{us}, 0_{ui}\rangle. \tag{2}$$

The nature of cascaded phase-matching is close to the quasi-phase-matching in periodically poled crystals. In Fig.1(c) the dependence of probabilities $|F_{s,i}|^2$, $|F_{us,i}|^2$ on the length of crystal is plotted. The probability of SPDC pairs $|1_s, 1_i, 0_{us}, 0_{ui}\rangle$ generation oscillates and at its maxima the increase of $|F_{us,i}|^2$ occurs. In this way we compensate wave-vector mismatch of SPDC by wave-vector mismatch of CUpC which results to efficient up-conversion and generation of IR-UV photon pairs $|0_s, 1_i, 1_{us}, 0_{ui}\rangle$ with suppressed contribution of pairs $|1_s, 1_i, 0_{us}, 0_{ui}\rangle$. The same consideration is valid for CUpC of idler photon. Besides, the fulfilment of both cascaded phase-matching conditions ($\widetilde{\Delta} = \Delta_s = \Delta_i$) allows one to generate spectrally entangled Bell states

$$|\Psi\rangle = F_{\text{vac}}|\text{vac}\rangle + F\Big(|0_s, 1_i, 1_{us}, 0_{ui}\rangle \pm |1_s, 0_i, 0_{us}, 1_{ui}\rangle\Big) \tag{3}$$

The generation of IR-UV photon pairs with the use of cascaded phase-matching has advantages before conventional schemes where SPDC and up-conversion occurs consistently in different nonlinear crystals. In conventional schemes conversion efficiency is sensitive to the pump power for frequency up-conversion and accompanied by additional quantum noise [6]. In CUpC such restrictions are absent that provides efficient noiseless up-converted states. Proposed approach can be implemented in heralded one-photon state generation in UV range.

This work is supported by RF President's Foundation for State Support of Young Russian Scientists (Grant No. MK-5886.2021.1.2).

References

[1] *C. Fabre and N. Treps*, Modes and states in quantum optics. Rev. Mod. Phys. **92**, 035005 (2020).

[2] *D. Klyshko*, Photons and Nonlinear Optics. (CRC Press, Boca Raton, FL, 1988).

[3] *S. M. Saltiel, A. A. Sukhorukov, and Y. S. Kivshar*, Multistep parametric processes in nonlinear optics. Progress in Optics, **43**, pp. 1–73 (2005).

[4] *A. V. Rasputnyi and D. A. Kopylov*, Quantum spatial dynamics of high-gain parametric down-conversion accompanied by cascaded up-conversion. Phys. Rev. A **104**, 013702 (2021).

[5] *J. Wei and E. Norman*, On Global Representations of the Solutions of Linear Differential Equations as a Product of Exponential. Proc. Am. Math. Soc. **15**, 327 (1963).

[6] *H. Rütz, K.-H. Luo, H. Suche, and C. Silberhorn*, Quantum Frequency Conversion between Infrared and Ultraviolet. Phys. Rev. Applied **7**, 024021 (2017).

Voronovo, Moscow, Russia November 9–12, 2021
4th International School on Quantum Technologies

Wigner function representation and efficient calculation method

Evgeny Burlakov[1*]

[1] *Faculty of Physics, Moscow State University, Moscow, Russia*
*E-mail: ev.burlakov@physics.msu.ru

Abstract

The Wigner function was first proposed by E. Wigner [[1]], and now is widely used in quantum tomography [[2]], quantum communication and cryptography [[3]], quantum informatics [[4]], in signal processing problems [[5]]. This research is devoted to a new method for calculating the Wigner function of an arbitrary quantum system with a potential in the form of a polynomial, using a new representation of the Wigner function in the form of an expansion in the basis of a harmonic oscillator.

Wigner function representation

Let a quantum system be described by a wave function Ψ for which the expansion (1) is valid:

$$\Psi(x,t) = \sum_{n=0}^{+\infty} c_n(t)\,\Psi_n(x), \tag{1}$$

where $\{\Psi_n\}$ is the harmonic oscillator eigenfunctions. The expansion coefficients $c_n = \int_{-\infty}^{+\infty} \bar{\Psi}_n(x)\,\Psi(x)\,dx$ correspond to the density matrix ρ ($\rho_{k,n} = c_k \bar{c}_n$, $\rho = \rho^{\dagger}$, $\mathrm{Tr}[\rho] = 1$). The Wigner function [[1]]:

$$W(x,p) = \frac{1}{2\pi\hbar}\int_{-\infty}^{+\infty} \exp\left(-i\frac{ps}{\hbar}\right)\left\langle x+\frac{s}{2}\right|\hat{\rho}\left|x-\frac{s}{2}\right\rangle ds\,, \tag{2}$$

is representable [[6]] as:

$$W(x,p) = \sum_{n,k=0}^{+\infty} \rho_{k,n} w_{n,k}(x,p) = \mathrm{Tr}\left[\rho\mathcal{W}(x,p)\right] = \bar{C}^T \mathcal{W} C, \tag{3}$$

$$w_{n,k}(x,p) = \frac{(-1)^n}{\pi\hbar} e^{-\kappa^2 x^2 - \frac{p^2}{\hbar^2\kappa^2}} \mathcal{P}_{n,k}\left(-\kappa x - i\frac{p}{\hbar\kappa}, \kappa x - i\frac{p}{\hbar\kappa}\right), \tag{4}$$

where $\kappa = \sqrt{\frac{m\omega}{\hbar}}$; $C = \{c_1, c_2, ...\}^T$. Polynomials $\mathcal{P}_{n,k}(z_1, z_2)$ have the form:

$$\mathcal{P}_{n,k}(z_1,z_2) = \sqrt{2^{n+k} n!k!} \sum_{s=0}^{\min(n,k)} \frac{z_1^{n-s} z_2^{k-s}}{2^s s!\,(k-s)!\,(n-s)!}. \tag{5}$$

Polynomial potential example

Using expressions (3) - (5), a method for constructing the Wigner function for a quantum system with a polynomial potential $U_N(x) = \sum_{n=1}^{N} a_n x^n$ of degree N was described in [[7]]. Let the wave function Ψ satisfy the Schrödinger equation $-\frac{\hbar^2}{2m}\Psi_{xx} + (U_N - \mathcal{E})\,\Psi = 0$ and admit expansion (1), then the vectors of the coefficients $C^{(\ell)}$ (3) are eigenvectors, and the energy spectrum $\mathcal{E}_\ell$ is the eigenvalues of the symmetric matrix $J_{n,k}$:

$$JC^{(\ell)} = \mathcal{E}_\ell C^{(\ell)}, \quad \ell \in N_0, \quad J_{n,k} = \langle\langle\varepsilon\rangle\rangle_n I^{(0)}_{n,k} + \sum_{l\neq 2}^{N} a_l I^{(l)}_{n,k}, \tag{6}$$

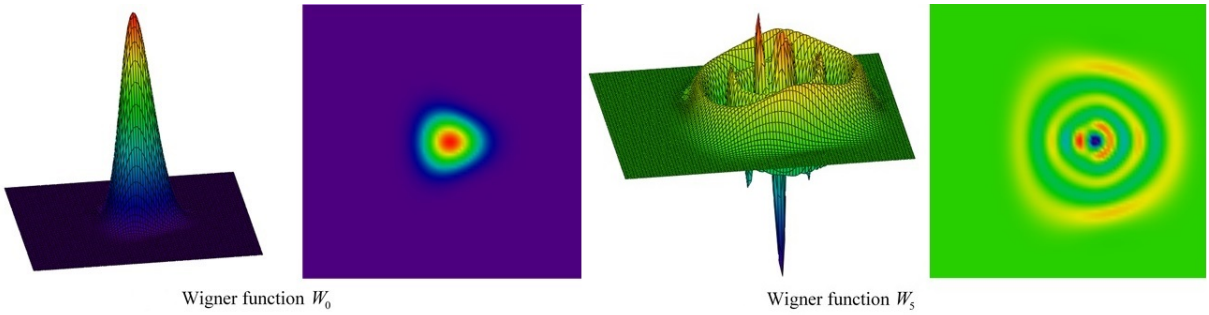

Figure 1: Wigner functions

$$I^{(l)}_{n,k} = \frac{l-1}{2\gamma} I^{(l-2)}_{n,k} + \sqrt{\frac{n}{2\gamma}} I^{(l-1)}_{n-1,k} + \sqrt{\frac{k}{2\gamma}} I^{(l-1)}_{n,k-1}, \;\; I^{(0)}_{n,k} = \delta_{n,k}, \;\; I^{(1)}_{n,k} = \sqrt{\frac{n}{2\gamma}} I^{(0)}_{n-1,k} + \sqrt{\frac{k}{2\gamma}} I^{(0)}_{n,k-1},$$

where $m\omega^2 = 2a_2$; $\gamma = \frac{m\omega}{\hbar}$; $\langle\langle\varepsilon\rangle\rangle_n = \hbar\omega\left(n + \frac{1}{2}\right)$ - energy spectrum of a harmonic oscillator.

Without loss of generality, we take $N = 5$, $a_l = \{0.01, 0.2, -1, 0, 2\}$. In Fig. 1 shows the Wigner functions constructed by the proposed method for the ground and fifth eigenstates.

Conclusion

For the quantum systems with polynomial potentials of the form $U_N(x)$ the proposed method by an order of magnitude reduces the Wigner functions computation time with the same accuracy compared to the numerical integration of expression (2). First, the use of explicit expressions (4) for matrix elements avoids direct numerical integration in expression (2). The functions (4) are known explicitly and for a fixed difference grid can be calculated once and stored in memory. Second, according to (6) the expansion coefficients form the eigenvectors of the matrix, the form of which is known exactly and can be calculated once before the start of the main calculation procedure. Fast exponential decay of $\{\Psi_n\}$ guarantees a small number of sum terms for acceptable approximation accuracy.

This work was supported by the RFBR grant No. 18-29-10014 and the Interdisciplinary Scientific and Educational School of Moscow State University. M.V. Lomonosov “Photonic and Quantum Technologies. Digital Medicine ”

References

[1] *E.P. Wigner*, On the quantum correction for thermodynamic equilibrium. Phys. Rev. **40**, (1932).

[2] *D.T. Smithey, M. Beck ,M.G. Raymer, A. Faridani*, Measurement of the Wigner distribution and the density matrix of a light mode using optical homodyne tomography: application to squeezed states and the vacuum. Phys. Rev. Lett. **70**, (1993).

[3] *A. Casado, S. Guerra, J. Plácido*, Wigner representation for experiments on quantum cryptography using two-photon polarization entanglement produced in parametric down-conversion. J. Phys. B At. Mol. Opt. Phys. **41**, 045501 (2008).

[4] *U. Andersen, J. Neergaard-Nielsen, P. van Loock et al.*, Hybrid discrete- and continuous-variable quantum information. Nature Physics. **35**, (2015).

[5] *T.A. Claasen, W.F. Mecklenbräuker*, The Wigner distribution—a tool for time-frequency signal analysis. II: discrete-time signals, part 2. Philips J. Res. **35**, (1980).

[6] *E.E. Perepelkin, B.I. Sadovnikov, N.G. Inozemtseva, E.V. Burlakov*, Explicit form for the kernel operator matrix elements in eigenfunction basis of harmonic oscillator. Journal of Statistical Mechanics: Theory and Experiment, 023109 (2020).

[7] *E.E. Perepelkin, B.I. Sadovnikov, N.G. Inozemtseva, E.V. Burlakov*, Wigner function of a quantum system with polynomial potential. Journal of Statistical Mechanics: Theory and Experiment, 023109 (2020).

Voronovo, Moscow, Russia November 9–12, 2021
4th International School on Quantum Technologies

Schrödinger cat states decoherence in a fiber quantum channel and their discrimination

Roman Goncharov[1,2*], **Fedor Kiselev**[1,2], **Natalia Veselkova**[1], **Alexei D. Kiselev**[1,2]

[1] *Quantum Information Laboratory, ITMO University, Kadetskaya Line, 3, Saint Petersburg, 199034, Russia*
[2] *Laboratory of Quantum Processes and Measurements, ITMO University, Kadetskaya Line, 3, Saint Petersburg, 199034, Russia*
*E-mail: rkgoncharov@itmo.ru

Abstract

In this work, we study the effect of decoherence in an optical fiber on the Schrödinger cat states from the standpoint of modern detection equipment. We calculate the fidelity and the photon counting probability on a segmented detector and discuss the potential implementation of such states for quantum communication systems.

Entanglement establishment is one of the main tasks of quantum communication protocols, including quantum repeaters. The use of the Schrödinger cat states in the context of the latter has been studied for quite a long time [1], however, a full-fledged experiment has not been implemented, and the reasons for this are not completely clear. The aim of this work is to assess the fragility of the cat states and their potential use in fiber channelsin the further context of quantum repeaters. For these purposes, we calculate the fidelity of symmetric and antisymmetric states for various decoherence parameters of the fiber channel. We then calculate the probability of state discrimination using the positive-operator-valued measure (POVM) of a realistic modern segmented single photon counting detector.

The object of our consideration is the following state

$$|\Psi\rangle_{\pm} = \frac{1}{\sqrt{M_{\pm}}}\left(|\alpha\rangle \pm |-\alpha\rangle\right), \tag{1}$$

$$M_{\pm} = 2(1 \pm e^{-2|\alpha|^2}). \tag{2}$$

We assume that decoherence procceses in the channels from Alice and from Bob to the central node are symmetric, we also consider a noisy channel through the introduction of an additional environmental mode as follows [2, 3]

$$|\Psi\rangle_{\pm} \to |\widetilde{\Psi}\rangle_{\pm} = \frac{1}{\sqrt{M_{\pm}}}\left(|\sqrt{\eta}\alpha\rangle\left|\sqrt{1-\eta}\alpha\right\rangle_E \pm |-\sqrt{\eta}\alpha\rangle\left|-\sqrt{1-\eta}\alpha\right\rangle_E\right), \tag{3}$$

where η denotes losses. For further considerations, we introduce a density matrix

$$\begin{aligned}
\rho_{\pm} &= \mathrm{Tr}_E\,|\widetilde{\Psi}\rangle_{\pm}\langle\widetilde{\Psi}| = \frac{N_+\widetilde{M}_{\pm}}{4M_{\pm}}|\widetilde{\Psi}'\rangle_{\pm}\langle\widetilde{\Psi}'| + \frac{N_-\widetilde{M}_{\mp}}{4M_{\pm}}|\widetilde{\Psi}'\rangle_{\pm},\langle\widetilde{\Psi}'|,\\
|\widetilde{\Psi}'\rangle_{\pm} &= \frac{1}{\sqrt{\widetilde{M}_{\pm}}}\left(|\sqrt{\eta}\alpha\rangle \pm |-\sqrt{\eta}\alpha\rangle\right),\\
\widetilde{M}_{\pm} &= 2(1 \pm e^{-2\eta|\alpha|^2}),\\
N_{\pm} &= 2(1 \pm e^{-2(1-\eta)|\alpha|^2}).
\end{aligned} \tag{4}$$

Now we are able to calculate the fidelity

$$F_{\pm} = {}_{\pm}\langle\Psi|\rho_{\pm}\,|\Psi\rangle_{\pm}\,. \tag{5}$$

For symmetric and antisymmetric cat states, respectively, we obtain

$$F_{+} = \frac{\cosh\left[(1-\eta)|\alpha|^2\right]}{\cosh^2|\alpha|^2}\left|\cosh[\sqrt{\eta}|\alpha|^2]\right|^2, \tag{6}$$

$$F_{-} = \frac{\cosh\left[(1-\eta)|\alpha|^2\right]}{\sinh^2|\alpha|^2}\left|\sinh[\sqrt{\eta}|\alpha|^2]\right|^2. \tag{7}$$

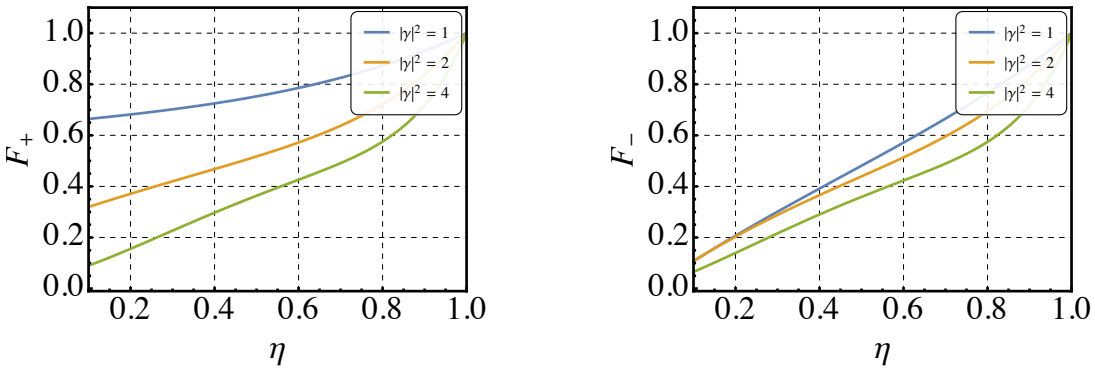

(a) (b)

Figure 1: Dependence of fidelity on the transmittance coefficient η for symmetric (a) and antisymmetric (b) states. Plots obtained for various mean photon numbers.

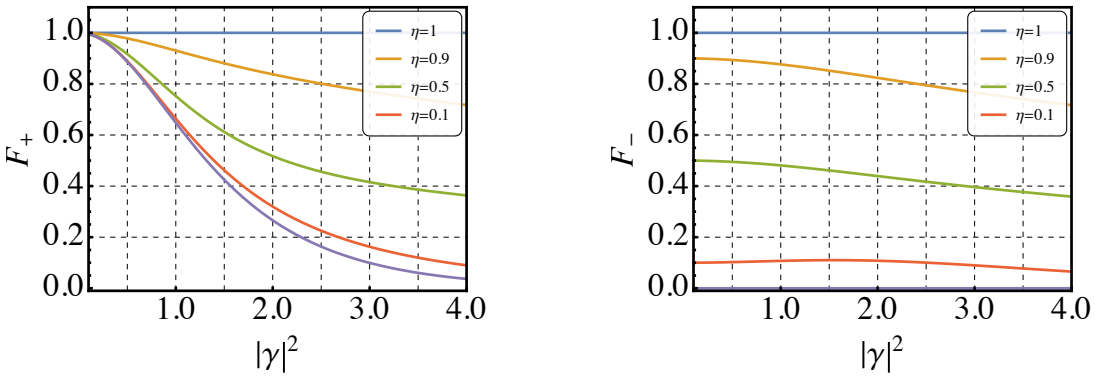

(a) (b)

Figure 2: Dependence of fidelity on the mean photon number for symmetric (a) and antisymmetric (b) states. Plots obtained for various η.

The behavior of the fidelity function with different set parameters can be seen in the Figures 1 and 2. The transition to unity for a symmetric cat state at zero amplitude is quite obvious, and this means that we are dealing with a vacuum state, which is not true under the same conditions in the antisymmetric case. It is also seen that in terms of entanglement creation, it is most preferable to use symmetric states at low amplitudes, since in this case, the fidelity is higher.

In order to provide cat state discrimination, it is necessary to use photon detectors that distinguish the parity of the number of arriving photons. Usually the more general problem of photon counting is posed. For further calculations, we consider a model of segmented detectors based on single-photon avalanche-photodiodes (SPAD) [4]. The POVM for such a detection system can be represented as follows

$$\Pi_k = \sum_{n=0}^{\infty} P(k \mid n)|n\rangle\langle n|, \tag{8}$$

where $P(k \mid n)$ conditional probability of k clicks in case of arrival of n photons. Taking into account the efficiency of detectors and dark counts,

$$P_m(k \mid n, \eta_{\text{loss}}, \delta) = n!(1-\delta)^m \left(\frac{1-\eta_{\text{loss}}}{m}\right)^n \binom{m}{k} \cdot \underbrace{\sum_{n_1=0}^{n} \cdots \sum_{n_m=0}^{n}}_{\sum_{j=1}^{m} n_j = n} \frac{1}{\prod_{j=1}^{m} n_j!} \prod_{l=n_1}^{n_k} \left[\frac{1}{1-\delta}\left(\frac{1}{1-\eta_{\text{loss}}}\right)^l - 1\right], \tag{9}$$

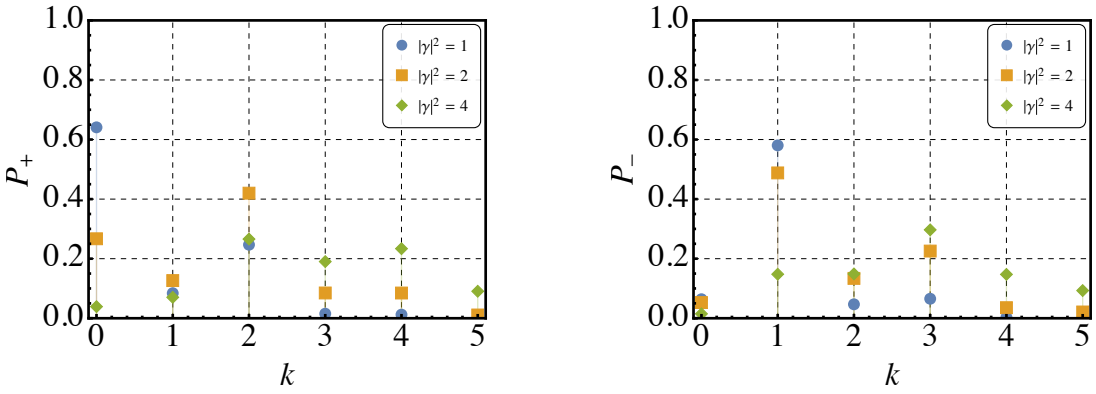

(a) (b)

Figure 3: Probability of photocounts to create the entanglement from symmetric (a) and antisymmetric (b) for a fixed value of $\eta = 1$.

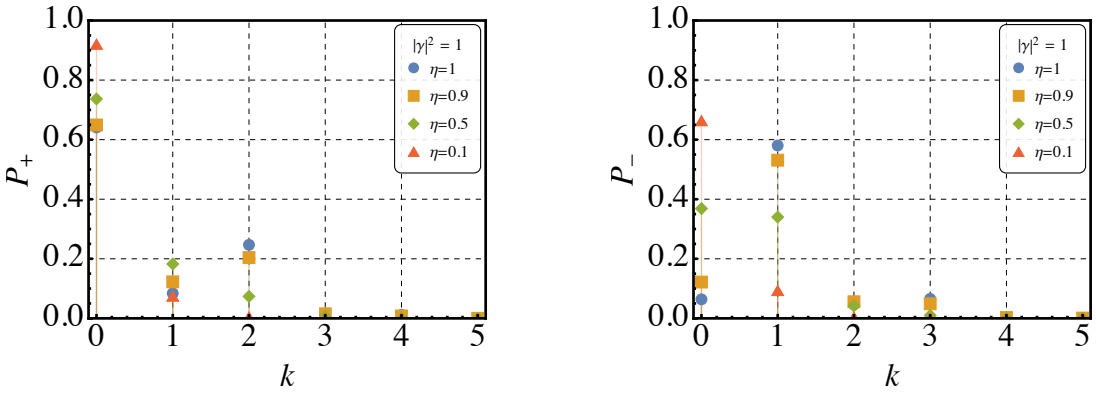

(a) (b)

Figure 4: Probability of photocounts to create the entanglement from symmetric (a) and antisymmetric (b) for a fixed mean photon number $|\alpha|^2 = 2$ at different values of η.

where m is a number of SPAD's, η_{loss} is a parameter describing the effect of photon losses in each detection mode, δ is a dark count probability.

To use the POVM, the given density matrix from Eq. (4) should be rewritten in the Fock basis

$$\rho_{\pm} = \frac{e^{-\eta|\alpha|^2}}{M_{\pm}} \left(N_{\pm} \sum_{n=0}^{\infty} \frac{(\eta|\alpha|^2)^{2n}}{(2n)!} |2n\rangle\langle 2n| + N_{\mp} \sum_{n=0}^{\infty} \frac{(\eta|\alpha|^2)^{2n+1}}{(2n+1)!} |2n+1\rangle\langle 2n+1| \right). \tag{10}$$

The following parameters were used for the calculation: $m = 16$, $\eta_{\text{loss}} = 0.9$, $\delta = 0.001$. From the Figures 3 and 4, we can again conclude that symmetric cat states are easier to distinguish. Moreover, the absence of a count for symmetric states can be interpreted as an even outcome, which in the antisymmetric case is undoubtedly an error. It is also seen that the probability of correct discrimination of states rapidly decreases with increasing distance due to decoherence. This, to some extent, speaks of the fragility of the cat states used. Nevertheless, we believe that the result can be improved: for example, the η_{loss} parameter can potentially be higher [4], as well as the number of detectors themselves. The latter has a strong effect on the computation time, so a smaller number was chosen.

Presented results shows that applicability of Schrödinger cat states for quantum communication protocols is challenging. In addition to the fact that the preparation of such states is a non-trivial task, their fragility plays a significant role when propagating in an optical fiber. However, the distribution of entangelement at short distances is possible. And, as stated, there is still some leeway to improve the component base for better discrimination.

References

[1] *N. Sangouard, C. Simon, H. De Riedmatten, and N. Gisin* Quantum repeaters based on atomic ensembles and linear optics. *Rev. Mod. Phys.* **83**, 33 (2011).

[2] *S.J. van Enk and O.Hirota* Entangled coherent states: Teleportation and decoherence. *Phys. Rev. A* **64**, 022313 (2001).

[3] *M. Ghasemi and M. Tavassoly* Toward a quantum repeater protocol based on the coherent state approach. *Laser Phys.* **29**, 085202 (2019).

[4] *R. Nehra, C.-H. Chang, Q. Yu, A. Beling, and O. Pfister* Photon-number-resolving segmented detectors based on single-photon avalanche-photodiodes. *Opt. Express* **28**, 3660–3675 (2020).

Voronovo, Moscow, Russia November 9–12, 2021
4th International School on Quantum Technologies

Implementation of Optical Quantum Memory in a Tm:YAG Crystal Waveguide

Aleksandr Pavlov[1*], **Mansur Minnegaliev**[1], **Konstantin Gerasimov** [1], **Evgeniy Moiseev** [1],**Timur Rupasov** [1], **Aleksandr Kalinkin** [2], **Sergei Kulik** [2], **Sergei Moiseev** [1]

[1] *Kazan Quantum Center, Kazan National Research Technical University n.a. A.N. Tupolev-KAI,Kazan, Russia*
[2] *Quantum Technologies Center and Faculty of Physics, M.V. Lomonosov Moscow State University, Moscow, Russia*
*E-mail: alex.pavlov@kazanqc.org

Abstract

The use of waveguide structures in a crystals doped with rare-earth ions is an interesting way in the development of an integrated QM. It was shown [1] that in Tm^{3+}:$Y_3Al_5O_{12}$ crystal it is possible to create 2x2 and 3x3 waveguide beam splitters with different power dividing ratios, which makes it possible to manufacture an optical chip with a given logic on one crystal. Earlier, in the Tm^{3+}:$Y_3Al_5O_{12}$ crystal, an optical QM protocol was implemented in a revival of silenced echo (ROSE) scheme with addressable writing and reading of input optical signals [2]. In this work an optical QM protocol was implemented in a Tm^{3+}:$Y_3Al_5O_{12}$ crystal single-mode waveguide. Such parameters as an absorption coefficient, coherence time, inhomogeneous broadening of the optical transition line of thulium ions in the waveguide structure and in a bulk crystal were experimentally determined. Also an optical QM protocol was experimentally implemented for weak light pulses in a ROSE scheme.

Crystal Tm^{3+}:$Y_3Al_5O_{12}$ with doping c=0.01 % and dimensions 2x9x19.5 mm is placed in a closed-cycle cryostat (Montana Instruments Corp.). The crystal is glued to cold finger of the cryostat with temperature 3.2±0.1 K by 3 mm thickness layer of silver paste. Twenty one type III single-mode waveguides were machined in the crystal along Z axis. Each waveguide is produced by femtosecond laser-writting 18 elliptical depressed cladding regions with axes of 2 and 8 μm around a circle with diameter of 18 μm. The produced waveguide has a Gaussian mode with half width half maximum of ~ 5.5 μm for both axis. The parameters of chosen single-mode waveguide are as follows: diameter - 18 μm , vertical polarization losses (parallel to 2 mm edge) - 0.66 dB/cm, horizontal losses(parallel to 19.5 mm edge) - 1.13 dB/cm. We defined optical transition absorption both for bulk crystal and a waveguide αL=0.266, αL= 0.12±0.04 respectively, where L=19.5 mm. We investigated absorption line of Tm ions transitions in a waveguide compared it to bulk crystal. Central absorption line is $\nu_0(\Gamma_{inhom})$=378.130 THz (793.377 nm) for bulk crystal and $\nu_0(\Gamma_{inhom})$=378.140 THz (793.356 nm) for the waveguide.

From the two-pulse photon echo decay we defined coherence (phase memory) time for bulk crystal T_M=72.2 μs (x=1.55) and waveguide T_M=63 μs (x=1.82).

In this work for the first time an optical QM protocol was implemented in a single-mode waveguide structure in a revival of silenced echo scheme in a Tm:YAG crystal. In the experiment, the recovery efficiency of input pulses was 0.5 % for a storage time of 30 μs. The storage of coherent optical pulses attenuated to the level of one photon in the reconstructed signal of the suppresses echo for a single signal-to-noise level has been achieved. Despite the use of rephasing pulses with amplitude and frequency modulation, with an increase in the area, the retrieval efficiency of the input signal decreased. This is explained by the effect of instantaneous spectral diffusion. The solution to this problem will make it possible to implement a quantum memory protocol in a suppressed echo signal reconstruction scheme for single-photon light fields with a high efficiency and signal-to-noise ratio.

References

[1] *N. Skryabin, A. Kalinkin, I. Dyakonov and S. Kulik*, Femtosecond Laser Written Depressed-Cladding Waveguide 2 × 2, 1 × 2 and 3 × 3 Directional Couplers in Tm^{3+}:YAG Crystal. Micromachines 11,1 (2020).

[2] *M. Minnegaliev, K. Gerasimov, R. Urmancheev, A. Zheltikov, S. Moiseev*, Linear Stark effect in Tm^{3+}:$Y_3Al_5O_{12}$ + crystal and its application in the addressable quantum memory protocol. Phys. Rev. B **103**, 174110, (2021).

Voronovo, Moscow, Russia November 9–12, 2021
4th International School on Quantum Technologies

Reconstructing linear-optical integrated circuits parameters through measurements of correlation functions of thermal fields

A V Romanova[1*], G V Avosopiants[1], K G Katamadze[1,2], Yu I Bogdanov[2], S P Kulik[1]

[1] *Quantum Technology Centre, Faculty of Physics, M. V. Lomonosov Moscow State University, Moscow, Russia*
[2] *Valiev Institute of Physics and Technology, Russian Academy of Sciences, Moscow, Russia*
*E-mail: romanova.av15@physics.msu.ru

Abstract

This work is devoted to the development and experimental testing of a method for characterization of linear-optical integrated circuits through measurements of correlation functions of thermal fields, which has high precision and is resistant to phase fluctuations at the inputs. The paper presents the results of numerical modeling of the proposed approach, as well as preliminary results of physical experiments.

In recent years, there has been an increasing interest in quantum computing. One of the platforms on which calculations can be implemented is the optical platform. The key element of such a platform is tunable integrated optical multichannel interferometers (chips). To perform precision calculations, it is necessary to know the exact parameters of the interference circuit. For this purpose, various methods of characterization of optical chips are used. The linear-optical transformation specified by the integrated circuit can be described by a transfer matrix M of dimension $m \times m$:

$$M = \begin{pmatrix} |M_{11}|\, e^{i\phi_{11}} & \dots & |M_{1j}|\, e^{i\phi_{1j}} & \dots \\ \dots & \dots & \dots & \dots \\ |M_{i1}|\, e^{i\phi_{i1}} & \dots & |M_{ij}|\, e^{i\phi_{ij}} & \dots \\ \dots & \dots & \dots & \dots \end{pmatrix}, \tag{1}$$

where $i, j = 1, 2, .., m$, and m — the number of input and output channels of the chip. This matrix connects the complex amplitudes of the input and output fields or annihilation operators: $E^{(out)} = ME^{(in)}$, $a^{(out)} = Ma^{(in)}$, where $E = [E_1, E_2, \dots, E_m]^T$, $a = [a_1, a_2, \dots, a_m]^T$. Since the reconstruction of the modules of the matrix elements is trivial (these are transmission coefficients), the reconstruction of phases is of greater interest.

Currently, there are two main methods of their reconstruction: using coherent [1] and two-photon states of light [2, 3]. However, their main problems are that the first one is unstable to phase fluctuations, and the second one requires too much measurement time.

The aim of this project is to develop and experimentally test a method that allows tomography of optical chips by means of thermal field interferometry. The advantage of this method, in comparison with others, is a simple scheme for preparing input states, relatively fast measurement time, as well as resistance to phase fluctuations.

To understand the basic idea, an analogy with Hanbury Brown-Twiss stellar interferometry may be useful, where second-order correlations are used (that is, correlations of intensities, not amplitudes) [4]:

$$g^{(2)} = \frac{\langle I_1 I_2 \rangle}{\langle I_1 \rangle \langle I_2 \rangle} \tag{2}$$

This made it possible to get rid of the blurring of the interference pattern due to various turbulences in the path of light.

In the proposed method, reconstructing a matrix of the form (1), we run thermal fields on each pair of inputs, then measure the correlation function on a pair of outputs. Using the properties of thermal fields, we approximate the data and obtain the desired phase.

To estimate the effectiveness of the approach, a comparison was made with the reference method of characterization of chips based on coherent states. First of all, numerical modeling of reconstruction experiments by two methods was carried out, during which it was shown that the presicion of reconstruction by the proposed method monotonically increases with increasing sample, and also demonstrated resistance to phase fluctuations, in contrast to the method using coherent states (Fig. 1).

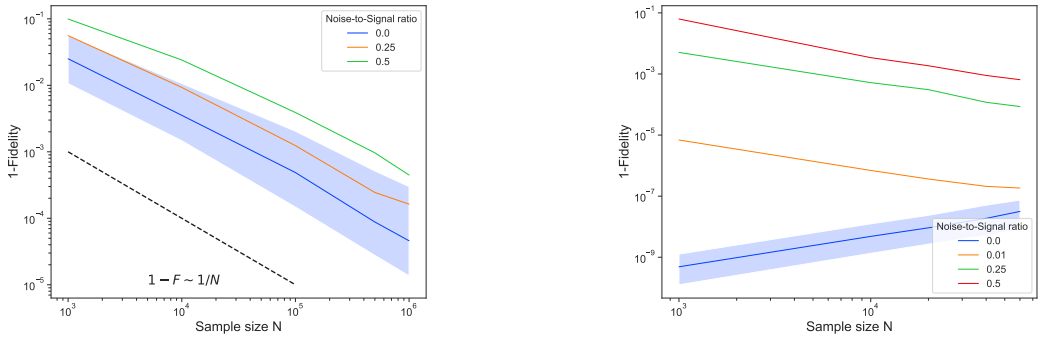

a) b)

Figure 1: Numerical modeling: a) thermal states, b) coherent states

Physical experiments were also carried out to reconstruct the unknown phase of the mounted optical circuit 2×2 by thermal and coherent states. Examples of the obtained data are shown in the figure 2.

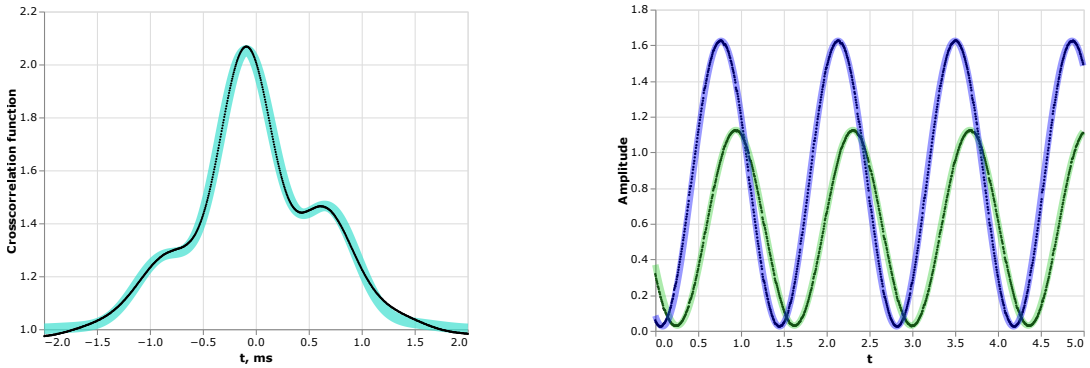

a) b)

Figure 2: Experimental data for $\phi \approx 45°$: a) thermal states, b) coherent states

Preliminary results for several circuit configurations are shown in the table 1:

Table 1: Reconstructed phases.

№	$\phi_{thermal}, ^\circ$	$\Delta_{thermal}, ^\circ$	$\phi_{coherent}, ^\circ$	$\Delta_{coherent}, ^\circ$
1	7.374762	0.321435	8.673547	0.006253
2	16.639479	0.020126	17.150462	0.011922
3	45.129335	0.124636	45.330506	0.036590
4	86.919155	0.232522	86.751116	0.036488
5	116.099952	0.124728	116.471307	0.049019
6	125.597496	0.314149	125.697662	0.026485
7	157.650275	0.112800	158.293362	0.014853
8	179.462526	0.180124	179.705495	0.001247

References

[1] S. Rahimi-Keshari, M. A. Broome, R. Fickler, A. Fedrizzi, T. C. Ralph, and A. G. White, "Direct characterization of linear-optical networks," *Optics Express*, vol. 21, no. 11, p. 13450, 2013.

[2] A. Laing and J. L. O'Brien, "Super-stable tomography of any linear optical device," *arXiv preprint arXiv:1208.2868*, 2012.

[3] N. Spagnolo, E. Maiorino, C. Vitelli, M. Bentivegna, A. Crespi, R. Ramponi, P. Mataloni, R. Osellame, and F. Sciarrino, "Learning an unknown transformation via a genetic approach," *Scientific reports*, vol. 7, no. 1, pp. 1–7, 2017.

[4] R. H. Brown and R. Q. Twiss, "Lxxiv. a new type of interferometer for use in radio astronomy," *The London, Edinburgh, and Dublin Philosophical Magazine and Journal of Science*, vol. 45, no. 366, pp. 663–682, 1954.

Voronovo, Moscow, Russia November 9–12, 2021

4th International School on Quantum Technologies

Implementation of revival of silenced echo memory protocol in $^{167}Er^{3+}:Y_2SiO_5$ crystal

Timur Sabirov[1*], Mansur Minnegaliev[1], Konstantin Gerasimov[1], Sergey Moiseev[1]

[1]*Kazan Quantum Center, KNRTU-KAI, Kazan, Russia*

*t.sabirov@kazanqc.org

Abstract

We demonstrated a photon echo quantum memory for weak input optical pulses on the revival of silenced echo memory protocol in a $^{167}Er^{3+}:Y_2SiO_5$ crystal. The quantum efficiency of 58% for a storage of time of 40 μs was achieved for single light pulses at telecom wavelength.

Active development of optical quantum technologies including optical quantum computing and long-range quantum communications stimulates the creation of quantum memory (QM). The creation of highly-efficient QM will not only significantly expand the capabilities of these technologies, but also leads to fundamental impact on the creation of new directions in their development [1]. In last decade, there was proposed and experimentally realized a number of protocols of QM. The schemes based on photon echo in solid state systems [2] demonstrated very promising results for achieving high quantum efficiencies and information capacity. Herein, the *revival of silenced echo* (ROSE) memory protocol seems especially attractive due to the possible use of natural inhomogeneously broadened line [2,3] that could significantly simplify practical implementation of QM. Another important task is the implementation of optical quantum memory for telecom wavelengths.

In this work we used $^{167}Er^{3+}:Y_2SiO_5$ crystal. The $^4I_{15/2} - {}^4I_{13/2}$ optical transition of erbium ions in the Y_2SiO_5 crystal is interesting because its wavelength λ = 1536 nm lies in the first optical transparency window of standard telecom fiber. Moreover, it possesses quietly long coherence time of optical transition 1.4 ms in external magnetic field and a typical inhomogeneous broadening of 500 MHz [1] . The presence of hyperfine sublevels for $^{167}Er^{3+}$ makes it possible to implement a long-lived spin-wave quantum memory, since the coherence time between them can reach 1 second, as was shown in the work [4].

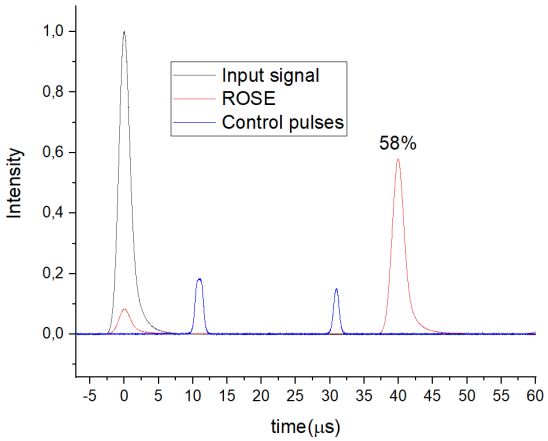

Figure 1: The signal of the revived silenced echo obtained by using $^{167}Er^{3+}:Y_2SiO_5$ crystal at time 40 μs. The signals from control pulses (red curve) can be seen between the input pulse and echo signal. At t=0 μs transmitted part of input pulse is shown by red. The echo signal recovery efficiency was 58% with storage time 40 μs.

A tunable single-frequency diode laser (Toptica CTL-1500) was tuned to a wavelength λ=1536.46 nm, corresponding to the $^4I_{15/2} - {}^4I_{13/2}$ transition (site 1). The $^{167}Er:Y_2SiO_5$ crystal with concentration of erbium ions c = 0.005 at. %. was placed inside closed-cycle cryostat with the superconducting magnet and cooled down to 1.3K. Input signal and control laser pulses propagated in opposite directions along the b axis of the crystal. In ROSE experiment shown in Fig. 1, we used a 2.4 μs Gaussian pulse (FWHM) as the input signal. The control pulses were with amplitude and frequency modulation and described as

$$\varepsilon(t) = \varepsilon_0 sech\big(\beta(t-t_0)\big) \qquad (1)$$
$$\omega(t) = \omega_0 + \mu\beta tanh\big(\beta(t-t_0)\big)$$

where μ and β define the frequency sweep range and the pulse duration.

In order to achieve the efficient rephasing one has to satisfy the adiabatic condition defined as $\mu\beta^2 \ll \Omega^2$, the damping should be small enough during the pulse duration $T_2\beta \gg 1$. The adiabatic conditions were fulfilled in our case with the following parameters β = 400 kHz and μ = 0.75 for storage of single input pulse with duration of 2.4 μs (FWHM). We implemented optical quantum memory ROSE protocol in this crystal with an efficiency of 55% for storage time of 40 μs. This is the largest efficiency that can be obtained for counter propagating geometry of signal and control pulses. Then we attenuated input pulse, so it contained about 90 photons. In this case, the retrieved echo signal contained about 45 photons for the signal-to-noise ratio of 1This caused by spontaneous emission noise caused by the remaining population in the excited state after the rephasing sequence. To evaluate the quality of rephasing pulses we implemented this memory scheme for different absorption values within the inhomogeneous profile and used following equation [5]:

$$\eta = (aL)^2 \cdot e^{-2\left(\frac{2\tau}{T_M}\right)^x} \cdot \eta_{phase}^2 \cdot e^{-\frac{aL(1+\eta_{pop})}{2}} \qquad (2)$$

Coefficients η_{pop}, η_{phase} are related to the return to the ground state (population) and the coherence rephrasing, respectively. The least square optimization gives $\eta_{phase} = 80\%$, $\eta_{pop} = 84\%$. These values are consistent and in good agreement with the experiments on luminescence intensity measurement after one and two control pulses.

Creating a useful device for quantum information applications will require ongoing efforts to improve efficiency and the quality of control pulses. Our experiment is an encouraging step towards demonstrating an optical quantum memory. These experiments confirms the possibility of using the ROSE protocol at the single photon level.

This research has been supported by Russian Science Foundation (project № 21-72-00115, https://rscf.ru/project/21-72-00115)

References

[1] *T. Böttger, C. W. Thiel, R. L. Cone, and Y. Sun,* Effects of magnetic field orientation on optical decoherence in Er^{3+}:Y_2SiO_5, Phys. Rev. B 79, 115104 (2009).

[2] *V. Damon, M. Bonarota, A. Louchet-Chauvet, T. Chaneli`ere, and J.-L. L. Gou¨et,* Revival of silenced echo and quantum memory for light. New Journal of Physics 13, 093031, (2011).

[3] *M. Bonarota, J. Dajczgewand, A. Louchet-Chauvet, J.-L. L. Gou¨et, and T. Chaneli`ere,* Large efficiency at telecom wavelength for optical quantum memories. Laser Physics 24, 094003, (2014).

[4] Rančić, M., Hedges, M. P., Ahlefeldt, R. L., & Sellars, M. J., Coherence time of over a second in a telecom-compatible quantum memory storage material. Nature Physics, 14(1), (2018).

[5] *Dajczgewand, J., Le Gouët, J. L., Louchet-Chauvet, A., & Chanelière, T.,* Large efficiency at telecom wavelength for optical quantum memories. Optics letters, 39(9), (2014).

Measurement of the normalized second-order correlation function for by photon fields by analog detectors

Daniil A. Safronenkov[1*], **Nadezhda A. Borshechevskaya**[1], **Tatiana I. Novikova**[1], **Konstantin G. Katamadze**[1,2], **Kirill A. Kuznetsov**[1], **Galiya Kh. Kitaeva**[1]

[1] *Lomonosov Moscow State University, Moscow, Russia*
[2] *Valiev Institute of Physics and Technology, Russian Academy of Sciences, Moscow, Russia*
*E-mail: safronenkov.da14@physics.msu.ru

Abstract

Experimental procedures are considered for measuring the second-order correlation function of the biphoton field, which is generated under spontaneous down conversion and detected by photon-counting and analog detectors. New approaches to processing of initially very noisy experimental data are analyzed. Three methods of successful eliminating electronic noises are proposed. These approaches can find their application in quantum technologies, for example, in the middle IR or terahertz frequency ranges.

Quantum-correlated pairs of optical photons (biphotons) are widely used in modern quantum technologies, from quantum communication [1], computing [2], to various types of quantum spectroscopy, imaging and sensing [3-5]. The normalized second-order correlation function $g^{(2)}$ is usually considered as a quantitative measure of the highest possible level of correlations in the process of spontaneous parametric down-conversion (SPDC).

We generate orthogonally polarized collinear frequency-degenerate biphotons by using type-II SPDC process in 41.2°-cut beta barium borate (BBO) crystal pumped at 405 nm. As a pump source, we used a spatially single-mode diode laser with a tunable power.

A comparison was made for values of the second-order correlation function obtained experimentally using 3 different detection methods. In the signal channel, there was always used a single-photon avalanche photo detector (APD№1) operating in the photon counting (method 1) or analogous (methods 2, 3) modes, and in the idler channel there was:
1) a single-photon counting APD operating in the photon counting mode (method 1),
2) a single-photon APD operating in the analog detection mode (method 2),
3) a detector based on a photo-multiple tube (PMT) which could operate in the analog mode only (method 3).

In the first case, the applied procedure was well known, and it was it that served for comparison the further obtained $g^{(2)}$ in the analog mode. In the second case, We replaced the APD samples with zero before processing the entire statistical set of APDs. We only replaced the low-level APD readings. This operation was performed for each APD. This procedure yielded the expected $g^{(2)}$ values. In the third case, three different discrimination methods were used to determine $g^{(2)}$ (Fig. 1) and quantum efficiency of the counting APD№1. The main problem was the correct recognition of the highly noisy PMT signal. The following methods were used to obtain the true $g^{(2)}$:
1) The first and simplest proposal was to use a method similar to the case with two APDs. However, this method did not give the desired result. Only at some currents was it possible to achieve $g^{(2)}$ close in value to that obtained in the counting mode.
2) We replaced PMT samples with zero before processing the entire PMT statistical set. We investigated various methods of such discrimination of PMT samples, but the simplest method was to remove low-level PMT samples. This method made it possible to obtain $g^{(2)}$ similar to the photon counting mode only at high values of the pump power.
3) In this method, we considered the distribution of the number of pulses from their amplitude. For APD, this dependence clearly shows the peak of noise currents. With the laser pumping off, it is possible to determine the low-level values of the currents that correspond to the APD noise. It is precisely from such dependences that the maximum value of the amplitude of the APD noise pulses can be determined. Then we zeroed out all values below the maximum value of the amplitude of the noise pulses in the APD and PMT channels. It was in this method that the true values of $g^{(2)}$ were obtained in the APD + PMT scheme and the absolute calibration of the APD№1 was carried out (Fig. 1).

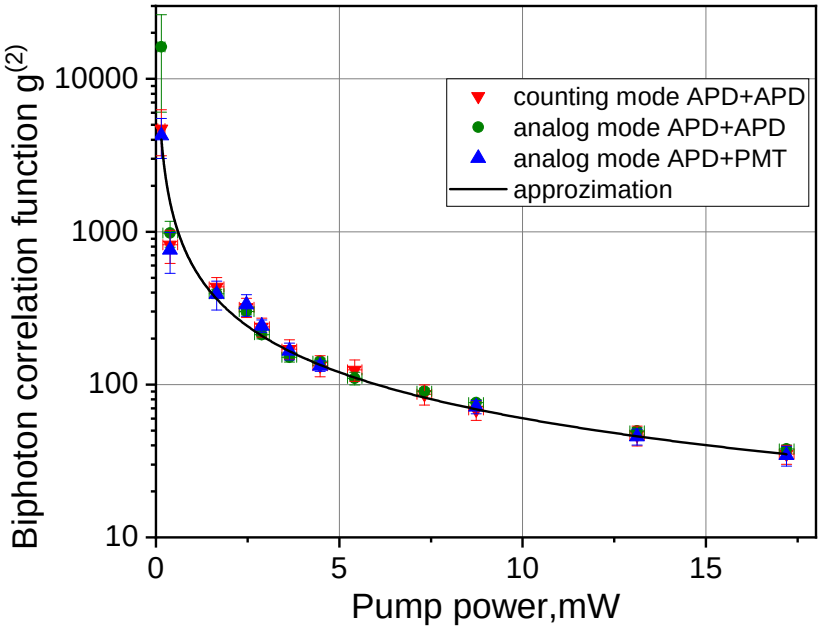

Figure 1: Values of the biphoton correlation function, determined experimentally at different powers of pump radiation by three detection systems: APD№1+APD№2 counting mode (red triangles), APD№1+APD№2 analog mode (olive circles), APD№1+PMT analog mode (blue triangles). Solid line: theoretical approximation for the correlation function dependence on the pump power with a single scaling coefficient.

In principle, this approach can be applied to measure the second-order correlation function when one or both photons are in the long-wavelength region [6].

Acknowledgements. We are grateful to Maria Chekhova, Pavel Prudkovskii for stimulating discussions and to Anton Konovalov for the technical help.

The study was performed under the support of the RFBR grant No. 19-02-00598 and the grant of Russian Science Foundation No. 17-12-01134

References

[1] *N. Gisin, and R. Thew*, Quantum communication Nat. Photonics **1**, 165-171 (2007).

[2] *F. Flamini, N. Spagnolo, and F. Sciarrino*, Photonic quantum information processing: a review. Rep. Prog. Phys. **82**, 016001 (2019).

[3] *G.B. Lemos, V. Borish, G.D. Cole, S. Ramelow, R. Lapkiewicz, and A. Zeilinger*, Quantum imaging with undetected photons Nat. **512**, 409 (2014).

[4] *P.-A. Moreau, E. Toninelli, T. Gregory, and M.J. Padgett*, Ghost Imaging Using Optical Correlations. Las. and Phot. Rev. **12**, 1700143 (2018).

[5] *A.V. Paterova and L.A. Krivitsky*, Nonlinear interference in crystal superlattices. Light: Science and Applications **9**, 82 (2020).

[6] *G. K. Kitaeva, A. A. Leontyev, and P. A. Prudkovskii*, Quantum correlation between optical and terahertz photons generated under multimode spontaneous parametric down-conversion. Phys. Rev. A **101**, 053810 (2020).

Voronovo, Moscow, Russia November 9–12, 2021
4th International School on Quantum Technologies

Atom chip for quantum sensing

A.E. Afanasiev[1,2], A.S. Kalmukov[1,2], R.V. Kirtaev[3], A.A. Kortel[1,2], P.I. Skakunenko[1,3,4*], D.V. Negrov[3], V.I. Balykin[1,2]

[1] *Institute of Spectroscopy Russian Academy of Sciences, Moscow, Troitsk, Russia*
[2] *National Research University Higher School of Economics, Moscow, Russia*
[3] *Moscow Institute of Physics and Technology, Dolgoprudny, Moscow Region, Russia*
[4] *Skolkovo Institute of Science and Technology, Moscow, Russia*
*E-mail: skakunenko.pi@phystech.edu

Abstract

We developed an atom chip and localized $3{\cdot}10^5$ atoms in U-shaped magneto-optical trap (U-MOT). Concentration and temperature of atoms are 10^{10} cm^{-3} and 200 μK respectively. After additional evaporative cooling the cloud of atoms will be exposed to a sequence of laser pulses to realize a quantum sensor of gravity.

Currently, many scientific groups around the world are creating and researching quantum sensors - devices for ultra-precise measurement of acceleration, rotational speed, gravitational forces, electromagnetic fields, and other physical quantities. Their work is based on the interference of the wave function of an atomic ensemble propagating along two different paths. This method is called atomic interferometry by analogy with conventional light interferometers. The result of interference depends on the phase difference between the two parts of the wave function, which, in turn, is determined by forces (inertial, gravitational, electromagnetic) acting on atoms.

Laser cooling of atoms allows monochromatization of atomic ensembles and precision control of internal degrees of freedom, which makes it possible to create quantum sensors with extreme sensitivity. In the future, they may have much higher accuracy and sensitivity compared to their classical analogs [1].

The most active direction in the field of creating quantum sensors based on cold atoms is the use of atom chips - devices that combine approaches of solid-state electronics and atom optics. This approach allows precise manipulation of neutral atoms at micro scales [2].

The purpose of our work is to create and study a gravimeter (a device for ultra-precise gravity measurement) based on atomic interference using atom chip technology. We developed an atom chip and managed to localize $3{\cdot}10^5$ Rubidium atoms in U-shaped magneto-optical trap (U-MOT) in high vacuum conditions. Reached concentration and temperature of atoms are 10^{10} cm^{-3} and 200 μK respectively. The trap was formed by intersecting laser beams and a constant electric current of 3A flowing through the silver micro wires of the atom chip. Further we plan to recapture these atoms into fully magnetic trap on the chip to additionally cool them via evaporative cooling. After that the cloud of atoms will be exposed to a sequence of laser pulses to realize a quantum sensor.

References

[1] *Degen, C. L., Reinhard, F., Cappellaro, P.*, Quantum sensing. Reviews of Modern Physics. 89(3) (2017).

[2] *R. J. Sewell, J. Dingjan, F. Baumgartner*, Atom chip for BEC interferometry. J. Phys. B: At. Mol. Opt. Phys. 43, 051003 (2010).

Voronovo, Moscow, Russia November 9–12, 2021
4th International School on Quantum Technologies

Matrix permanents in statistical physics of many-body quantum systems

Sergey Tarasov[1*], **Vladimir Kocharovsky**[1], **Vitaly Kocharovsky**[1,2]

[1] *Institute of Applied Physics RAS, Nizhny Novgorod, Russia*
[2] *Department of Physics and Astronomy, Texas AM University, College Station, TX, USA*
*E-mail: serge.tar@gmail.com

Abstract

We have found that describing the quantum statistics of a many-body system can often be reduced to calculating a permanent of some matrix. In particular, we present such a reduction for the Ising model of an arbitrary dimension and for the problem of finding the joint probability distribution of the number of atoms occupying different excited states in a Bose-condensed gas. Calculating a permanent of an arbitrary matrix is believed to be ♯P-complete problem, which means it belongs to the class of the hardest problems accessible to universal quantum computing, so that its solution gives a key to solutions of any other ♯P-problem. Thus, considered many-body systems may be viewed as an oracle on which a quantum computing device is based. We discuss these avenues in conjunction with finding an approximation/asymptotics for a matrix permanent and reveal a connection of the permanent with many areas of physics and mathematics, such as critical phenomena in phase transitions, quantum computing, quantum information processing, cryptography, fractal geometry, chaos theory, number theory, and theory of computational complexity. We suggest to employ the matrix permanent as a convenient tool for a unified description of the complexity of different systems and for an implementation of the ♯P-oracle in quantum computing.

The permanent of a $n \times n$ matrix (A_{pq}), being a function of matrix entries, is equal to the sum of all possible products of the entries, one from each row and one from each column of the matrix:

$$\operatorname{per} A = \sum_{\sigma \in S_n} \prod_{p=1}^{n} A_{p\,\sigma(p)} \ , \qquad \det A = \sum_{\sigma \in S_n} \operatorname{sgn}(\sigma) \prod_{p=1}^{n} A_{p\,\sigma(p)}; \tag{1}$$

here σ are permutations of the symmetric group S_n. In many-body physics, the permanent appears naturally since it represents a many-particle wave function in a system of n Bose particles as a symmetrized product of the single-particle wave functions. It is known in quantum field theory as the Caianiello permanent and is similar to the Slater determinant which represents a many-particle wave function in a system of n Fermi particles.

The definition of the permanent looks similar to the one of the matrix determinant, except the factor $\operatorname{sgn}(\sigma)$ isn't involved. However, due to this difference permanents are much more complex objects to deal with – they are not invariant under nontrivial transformations of basis (except ort permutations or coordinate rescaling). Computing the permanent of an arbitrary matrix is believed to be a ♯P-hard problem, which cannot be effectively implemented on a classical computer since the complexity of calculations grows exponentially with the size of the matrix (for example, the Ryser algorithm, one of the most efficient among the known ones, has the complexity of $n^2 2^n$). Moreover, it is a ♯P-complete problem [1], which means that for any problem in the ♯P-complexity class there is a deterministic polynomial-time Turing reduction to a counting problem according to the Toda's theorem [2].

According to the latter remark, finding many-body quantum systems, observables of which are directly associated with permanents of nontrivial matrices sseems to be a very intriguing task. On one hand, such systems – in the case of well-controllable associated matrices – may be considered as ♯P-complete oracles for the universal quantum computer. In fact, a polynomial-time machine only needs to make one ♯P-query to the oracle in order to calculate effectively any task belonging to the ♯P class. On the other hand, finding such systems is also important for analyzing the complexity of modeling and calculating specific characteristics of quantum systems using classical computers.

Based on a microscopic analysis of many-body quantum statistics, we present two novel examples of quantum systems, characteristics of which may be reduced to permanents. The method involves multivariate characteristic functions of probability theory and the Fourier transform theory; such a technique

links the expectation values (which are by definition 'observables' in quantum mechanics) to the derivatives of the characteristic function (see [3]). Thus, applying the method to the many-body system and associating each characteristic function argument to, say, occupation numbers of different boson modes of the analyzed systems, one surely should expect correlation functions (and related characteristics) to be in the essential form of the matrix permanent due to the famous MacMahon master theorem, which comes from linear algebra and enumerative combinatorics.

The first example presented is a calculation of a joint probability distribution for the particle occupation numbers in a Bose-Einstein-condensed gas confined in a mesoscopic trap. This joint probability distribution has been linked to the permanent of a unitary matrix transforming particles to the Bogoliubov quasiparticles. The obtained statistics has a lot in common to the one realized for BosonSamplers, which are well-known linear optical systems, frequently considered as demonstrators of quantum supremacy of the many-body interacting systems for computing [4].

The second example is a many-body spin lattice. Namely, for an arbitrary dimension Ising model considered as a generic model of the critical phenomena we found the reduction of the partition function and the order parameter to the matrix permanents [5]. The result is based on a bosonization of a many-body constrained system via a Holstein-Primakoff representation of spins. According to this procedure each spin is associated with the 2-level system of a fixed number of noninteracting Bose-particles, which makes the canonical-ensemble analysis of the Bose-condensate relevant to studies of the Ising problem. The matrix appearing in the obtained solution corresponds to the unconstrained Bose problem which is much easier to solve than the initial problem of interacting spins.

We also probe different ways of finding an approximation/asymptotics of the large-size permanents and reveal curious connections of the permanent with many areas of physics and mathematics. In particular, representations of the permanent based on the mode selection idea leads to integrals, Weierstrass-like kernels of which have a self-similar hierarchy of maxima (the overall depth of that hierarchical structure is limited by the finite size of the matrix). Thus, the accumulation of the integral approximating the permanent essentially has a fractal nature, which may be analyzed in terms of nontrivial Hausdorff dimensions. The decomposition of an arbitrary circulant matrix to a sum of the (degenerate) Schur or Fourier matrices, massively used in innumerable calculating applications, throws the bridge to the number theory: the contribution from each Schur matrix in this decomposition is characterised by special functions closely related to the well-known Euler's totient function and the Möbius function. At last, even calculating permanents of toy model objects leads to nontrivial results; e.g., the investigation of permanents of Toeplitz matrices with 1, 2 or 3 any-value diagonals on top of a uniform matrix allows us to derive in a much simpler and transparent way recursive relations for the 3-ménage numbers, famous in enumerative combinatorics.

To conclude, we infer that the permanent may be a convenient tool for a unified description of the complexity of different systems as well as for implementation of the ♯P-oracle in quantum computing.

The presented results were obtained with the support of the Foundation for the Advancement of Theoretical Physics and Mathematics "BASIS" (project # 20-1-3-50-1).

References

[1] *L.G. Valiant*, The Complexity of Computing the Permanent. Theoretical Computer Science **8**, 189 (1979).

[2] *S. Toda*, PP is as Hard as the Polynomial-Time Hierarchy. SIAM J. Comput. **20**, 865 (1991).

[3] *S.V. Tarasov, V.V. Kocharovsky, Vl.V. Kocharovsky*, Bose-Einstein-condensate fluctuations versus an interparticle interaction. Physical Review A **102**, 043315 (2020).

[4] *S. Aaronson, A. Arkhipov*, The computational complexity of linear optics. Theory of Computing **9**, 143 (2013).

[5] *V.V. Kocharovsky, Vl.V. Kocharovsky, S.V. Tarasov*, Unification of the Nature's Complexities via a Matrix Permanent – Critical Phenomena, Fractals, Quantum Computing, #P-Complexity. Entropy **22**, 322 (2020).

Voronovo, Moscow, Russia November 9–12, 2021
4th International School on Quantum Technologies

Countermeasure to laser damage attack based on neutral-density filter

Sergei Alferov, Kirill Bugai, Ivan Pargachev

JSC "InfoTeCS", Moscow, Russia
*E-mail: Sergey.Alferov@infotecs.ru

Abstract

The majority of quantum key distribution (QKD) systems are based on the use of weak coherent laser pulses. The mean photon number in pulses must be preset to ensure the security of key distribution. The pulses are attenuated to a single-photon level using an optical attenuator. A laser damage attack (LDA) can decrease attenuation of the optical attenuator, and the assumption about the mean photon number may be violated. As a result, an eavesdropper can then compromise the security of the QKD system. The authors of this report experimentally tested protection against LDA using a neutral-density filter. Experimental data and analysis will be presented at the conference.

Introduction

Traditionally, the security of quantum key distribution is associated with fundamental laws of quantum mechanics. However, the practical implementation often has flaws and equipment imperfections that create vulnerability. There are a number of articles describing such vulnerabilities [1, 3]. QKD systems often employ optical pulses attenuated to a single-photon level using an optical attenuator. The article [4] reveals some types of LDA-resistance attenuators. However, it shows its functions only when duration and power limitation of laser assumption criteria are met. Thus, the task of searching and creating optical elements unaffected to LDA is actual.

Experimental setup and testing method

The test of the optical attenuator (DUT) was conducted using the setup shown in Fig. 1.

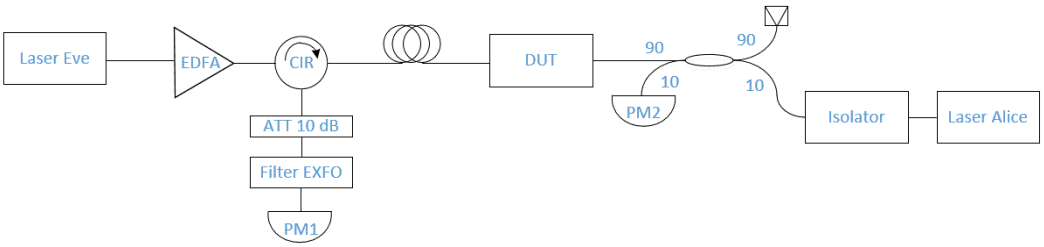

Figure 1: Experimental setup

The experimental setup mimics the LDA-scenario [4] for a real QKD system. A hacking laser consisted of a seed laser and an erbium-ytterbium-doped fiber amplifier (EDFA). A fiber-pigtailed laser was used as a seed source for the EDFA. The amplifier EDFA provided up to 37.4 dB cw power (λ =1561 nm). A laser Alice was a fiber-pigtailed 1547.3-nm laser that provided 18 dBm cw power. A power meter PM1 (Thorlabs 154-C) measured Alice's laser optical power after the attenuator (DUT). A power meter PM2 (Thorlabs 146-C) checked Alice's laser optical power before the DUT. An EXFO flirter served for elimination reflected radiation of Eve's laser on PM1. The optical attenuator consisted of a fiber bench (Oz Optics RFF-11-1550-9/125) with two collimating lenses that had numerical aperture NA=0.14. A collimated beam was attenuated by a neutral density filter (NDF). The filter was made of a glass plate with optical density OD=3.0 and a two-side coating of metal-dielectric layers.

The testing procedure was the following. At first, the power meter PM1 measured the optical power of Alice's laser at the calibration phase. It was done without Eve's laser. Then, the Alice's laser was blocked, and the Eve´s laser was activated to measure background noise, namely, it reflected and scattered light. Power range of Eve's laser was from 25 to 37.4 dBm. It turned out that initially measured attenuation of NDF was 36.34 dB. The highest power of background noise from Eve's laser on PM1 was -56.2 dBm. The signal-to-noise ratio was at least 22.4 dB, so that the noise component could be neglected in the calculations. After the calibration phase, both lasers were activated, and measurements of NDF attenuation at different Eve's laser powers were conducted. The attenuation was determined by comparing the power meter readings PM1 and PM2 (taking into account 10 dB attenuation of the 90:10 beam splitter and other losses).

The variation of filter attenuation depending on Eve's laser power is shown in Fig. 2.

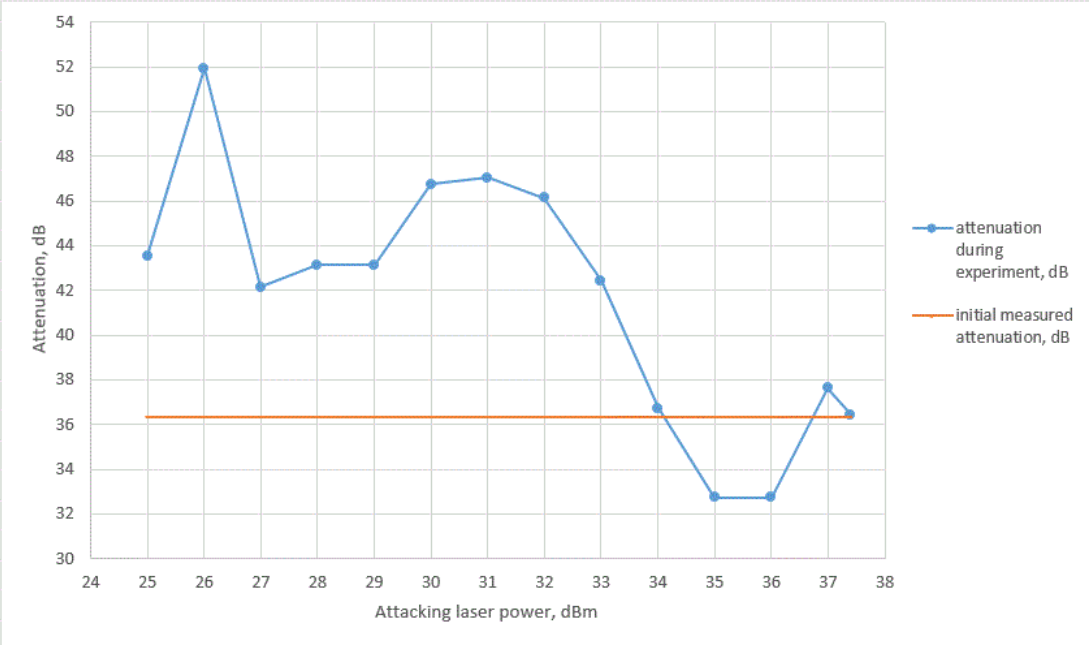

Figure 2: The variation of filter attenuation versus Eve's laser power

Accumulation time and time step were 60 s and 10 ms respectively. The horizontal line indicates initially measured attenuation before the application of high power. The graph shows that the filter attenuation is not constant when Eve's laser power is above 34 dBm becomes lower than the initial level. A temporal dependence of filter's attenuation for 10 seconds is shown in Fig. 3.

The dependence demonstrates a sharp gain of attenuation. The explanation of this Fig. 4 can be coating degradation that was accompanied by ablation and cracking.

The attenuation reverted to the initial state after the experiments. It can be explained by the cooling down of the filter and fiber bench.

Conclusion

Experiments have shown that NDF with a two-side coating of metal-dielectric layers is vulnerable to the laser-damage attack at powers above 34 dBm. The permanent degradation of NDF filter caused by the high-power cw laser was detected. Further research will be carried out with bulk-tinted filters. These filters absorb optical power throughout the entire volume, so it can be expected that their resistance to attack will be higher.

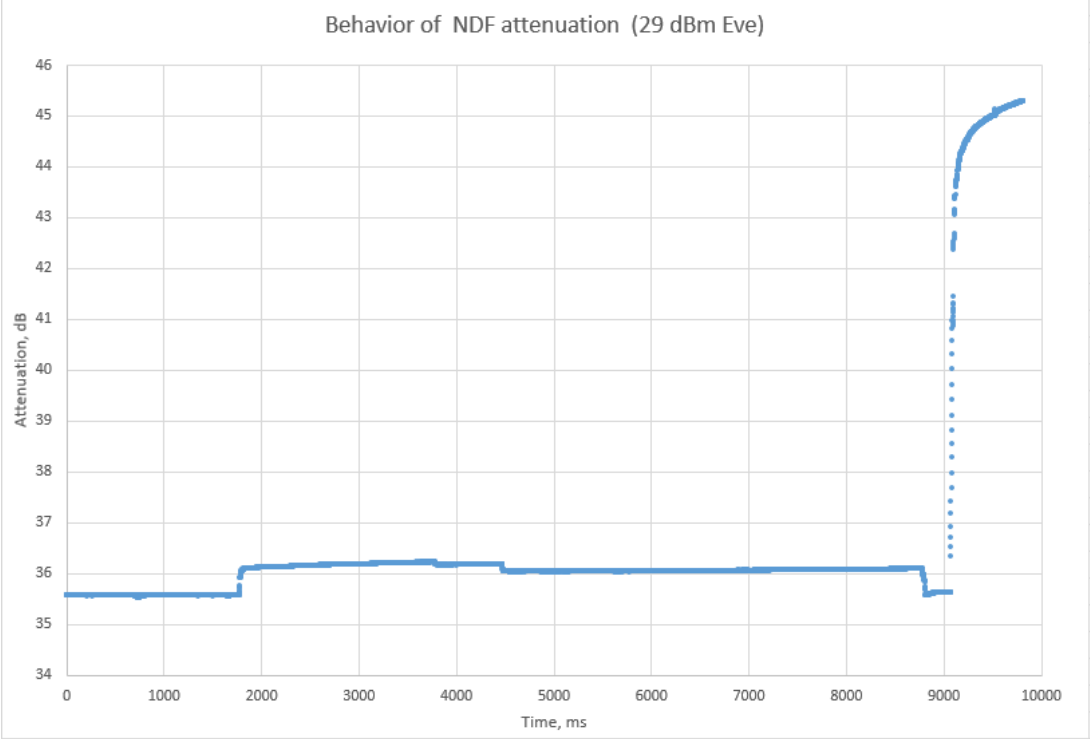

Figure 3: The variation of filter attenuation versus Eve's laser power

Figure 4: The surface of filter after experiments

References

[1] *A. Lamas-Linares and C. Kurtsiefer*, Breaking a quantum key distribution system through a timing side channel. Opt.Express **15**, 9388 (2007).

[2] *Shihan Sajeed, Igor Radchenko, Sarah Kaiser, Jean-Philippe Bourgoin, Anna Pappa, Laurent Monat, Matthieu Legré, and Vadim Makarov*, Attacks exploiting deviation of mean photon number in quantum key distribution and coin tossing. Phys. Rev. A. **91**, 032326 (2015).

[3] *F. Xu, B. Qi, and H.-K. Lo*, Experimental demonstration of phase-remapping attack in a practical quantum key distribution system. New J. Phys. **12**, 113026 (2010).

[4] *A. Huang, R. Li, V. Egorov, S. Tchouragoulov, K. Kumar and V. Makarov*, Laser-Damage Attack Against Optical Attenuators in Quantum Key Distribution. Phys. Rev. Appl. **13**, 034017 (2020).

Voronovo, Moscow, Russia November 9–12, 2021
4th International School on Quantum Technologies

Nanoindentation-based approach to integration of quantum emitters in 2D materials with nanophotonic structures

Artem Abramov[1*], **Ivan Iorsh**[1], **Mihail Petrov**[1], **Vasiliy Kravtsov**[1]

[1] *Department of Physics, School of Physics and Engineering, ITMO University, Russia*
*E-mail: artem.abramov@metalab.ifmo.ru

Abstract

In this work, we investigate a new approach to create single-photon emitters (SPEs) based on nanoindentation of 2D materials with an atomic force microscope probe. We experimentally show the possibility of precise positioning of 2D materials-based SPEs on a chip and the single-photon nature of their radiation. Further, we perform numerical simulations that demonstrate the possibility of controlling the frequency and radiation pattern of SPEs using resonant nanostructures.

1. Introduction

Individual photons are very promising as carriers of quantum information. Single-photon emitters are therefore important elements of quantum optoelectronics with applications in quantum computing and quantum communications devices. For the practical use of advanced quantum information processing systems, it is necessary to develop single photon emitters capable of operating with fast emission rates and characterized by high extraction efficiency. This can be achieved by integrating SPE with nanophotonic structures on a chip.

Two-dimensional materials provide a promising platform for hosting single-photon emitters [1]. However, integration of such quantum emitters with nanophotonic structures for practical use in on-chip devices remains challenging. Here we demonstrate a new approach based on nanoindentation of 2D materials with an atomic force microscope probe in the vicinity of nanophotonic structures. The approach relies on creating strong local strain fields in the crystal lattice of the 2D material and locally changing its band structure [2], leading to the formation of single-photon emitters. This also allows control on the coupling between single-photon emitters and photonic structures via deterministic placement of emitters in the near-field of the structure.

2. Experimental

Our structure is a WSe_2 monolayer placed on top of a deformable polymer film with nanophotonic structures located underneath (Fig. 1a). The monolayer is indented with a specially modified Si probe, leading to permanent local deformation due to the adhesion at the monolayer/polymer interface [3]. Quantum emitters are created and localized at the nanoindents and exhibit emission with radiation lines in the range of 750–850 nm (Fig. 1b). We verify the single-photon character of the fabricated emitters via second order correlation function measurements yielding the second-order correlation function value at zero delay $g^{(2)}(0)$ close to 0.15 (Fig. 1c).

Bull's eye resonators are nanophotonic structures well suited for controlling the radiation pattern and emission amplification due to the Purcell effect [4, 5]. Our numerical modeling of an "SPE – bull's eye resonator" structure (Fig. 2) shows that coupling of the SPE and Au resonator can result in enhanced emission rate and intensity with Purcell factors up to 20 (Fig. 3a). Integration of SPE with the resonator also changes the radiation pattern of the SPE, which will allow more efficient collection of the emission in the far-field (Fig. 3b,c).

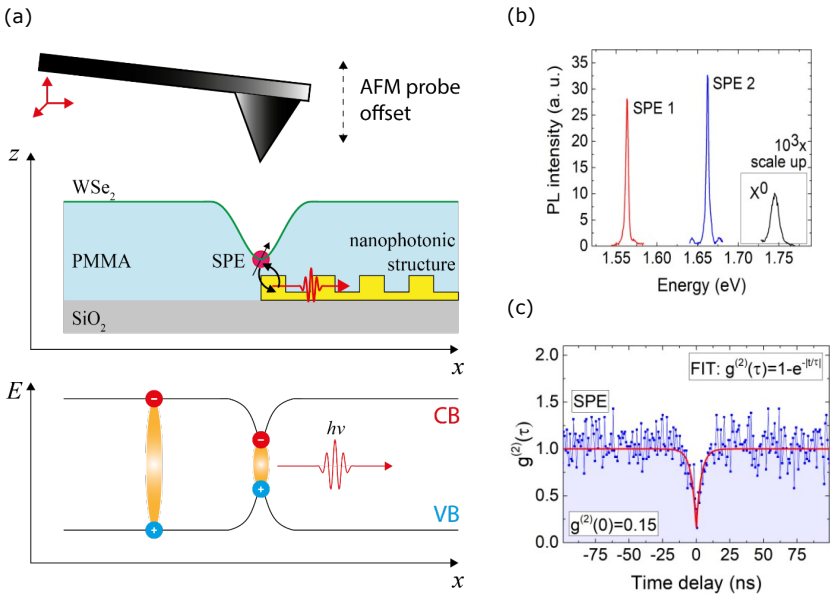

Figure 1: (a) Concept image of SPE fabrication approach based on nanoindentation of WSe_2 monolayer with an atomic force microscope probe. Schematic showing a single exciton trapping from the reservoir in 2D WSe_2 into a strain-induced potential minimum, giving rise to the non-classical light red-shifted from the emission in the unstrained monolayer. (b) PL spectrum of two selected SPEs and PL spectrum of a neutral exciton of WSe_2 monolayer ($T = 7$ K). (c) Experimentally measured second order correlation function for the PL signal from SPE.

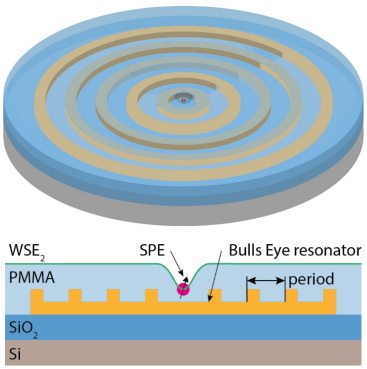

Figure 2: Concept image of an SPE integrated with a bull's eye structure (top view and side view).

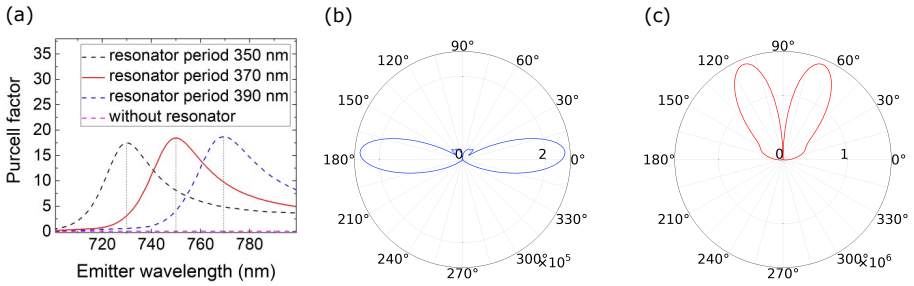

Figure 3: (a) Dependence of the Purcell factor from the wavelength of SPE and period of the resonator. (b) Radiation pattern of SPE without a resonator. (c) Radiation pattern of SPE integrated with a resonator (out-of-plane position of dipole).

3. Conclusion

Our experimental results and numerical simulation show that the nanoindentation-based approach to integrating quantum emitters in 2D materials with nanophotonic structures is promising for achieving single-photon emission with increased brightness, decreased lifetimes, and optimized directivity. The results of our research work are important for future applications in photonic engineering, quantum computing, and quantum communications.

References

[1] *M. Toth, I. Aharonovich*, Single photon sources in atomically thin materials. Annu. Rev. Phys. Chem. **70**, (2019).

[2] *F. A. Benimetskiy, V. A. Sharov, P. A. Alekseev, V. Kravtsov, K. B. Agapev, I. S. Sinev, I. S. Mukhin, A. Catanzaro, R. G. Polozkov, E. M. Alexeev, A. I. Tartakovskii, A. K. Samusev, M. S. Skolnick, D. N. Krizhanovskii, I. A. Shelykh, and I. V. Iorsh*, Measurement of local optomechanical properties of a direct bandgap 2D semiconductor. APL Materials. **7**, 10 (2019).

[3] *M. R. Rosenberger, C. K. Dass, H. J. Chuang, S. V. Sivaram, K. M. McCreary, J. R. Hendrickson, and B. T. Jonker*, Quantum calligraphy: writing single-photon emitters in a two-dimensional materials platform. ACS nano. **13**, 1 (2019).

[4] *S. K. H. Andersen, S. Bogdanov, O. Makarova, Y. Xuan, M. Y. Shalaginov, A. Boltasseva, S. I. Bozhevolnyi, and V. M. Shalaev*, Hybrid plasmonic bullseye antennas for efficient photon collection. Acs Photonics. **5**, 3 (2018).

[5] *S. Xia, T. Aoki, K. Gao, M. Arita, Y. Arakawa, and M. J. Holmes*, Enhanced Single-Photon Emission from GaN Quantum Dots in Bullseye Structures. ACS Photonics. **8**, 6 (2021).